NAVAL POSTGRADUATE SCHOOL

MONTEREY, CALIFORNIA

THESIS

SPECTRAL SHAPING AND SYMBOL ERROR MITIGATION TECHNIQUES TO INJECT OFDM SUBCARRIERS INTO NAVIGATIONAL RADAR GUARD BANDS AND MAINLOBE FOR SPECTRUM SHARING

by

Michelle L. Parmentar

March 2019

Thesis Advisor: Ric Romero
Second Reader: Tri T. Ha

Approved for public release. Distribution is unlimited.

THIS PAGE INTENTIONALLY LEFT BLANK

REPORT DOCUMENTATION PAGE			*Form Approved OMB No. 0704-0188*

1. AGENCY USE ONLY *(Leave blank)*	**2. REPORT DATE** March 2019	**3. REPORT TYPE AND DATES COVERED** Master's thesis

4. TITLE AND SUBTITLE SPECTRAL SHAPING AND SYMBOL ERROR MITIGATION TECHNIQUES TO INJECT OFDM SUBCARRIERS INTO NAVIGATIONAL RADAR GUARD BANDS AND MAINLOBE FOR SPECTRUM SHARING	**5. FUNDING NUMBERS**
6. AUTHOR(S) Michelle L. Parmentar	
7. PERFORMING ORGANIZATION NAME(S) AND ADDRESS(ES) Naval Postgraduate School Monterey, CA 93943-5000	**8. PERFORMING ORGANIZATION REPORT NUMBER**
9. SPONSORING / MONITORING AGENCY NAME(S) AND ADDRESS(ES) NCWDG, Suitland, DC 20395	**10. SPONSORING / MONITORING AGENCY REPORT NUMBER**

11. SUPPLEMENTARY NOTES The views expressed in this thesis are those of the author and do not reflect the official policy or position of the Department of Defense or the U.S. Government.

12a. DISTRIBUTION / AVAILABILITY STATEMENT Approved for public release. Distribution is unlimited.	**12b. DISTRIBUTION CODE** A

13. ABSTRACT (maximum 200 words)

In this work, we investigate the effects of spectrally opportunistic shaped communications waveforms impinging into the spectrum of a radar. To simulate the radar, we first use a Hamming-based spectral shape and a more realistic spectrum from a commercial navigation (COMNAV) radar. The communications system employs orthogonal frequency-division multiplexing (OFDM) with the subcarriers modulated by quaternary phase-shift keying (QPSK). We utilize waterfilling, adhoc waterfilling inversion, and uniform energy distribution techniques to shape the communications spectrum, fill the spectral tails (i.e., guard bands), and even inject subcarriers into the radar bandwidth. Unsurprisingly, the high-powered radar interferes with the communications signal such that the symbol error ratio (SER) is drastically degraded. In addition to the spectral shaping techniques on transmit, we propose estimation and subtraction of the radar interference from the interfered subcarriers. The combination results in SERs that are vastly improved, while the radar probability of detection is minimally or slightly affected.

14. SUBJECT TERMS communications, interference, probability of detection, radar, spectrally-shaped waveform, spectrum sharing, spectrum management, symbol error rate, bit error rate	**15. NUMBER OF PAGES** 75
	16. PRICE CODE

17. SECURITY CLASSIFICATION OF REPORT Unclassified	**18. SECURITY CLASSIFICATION OF THIS PAGE** Unclassified	**19. SECURITY CLASSIFICATION OF ABSTRACT** Unclassified	**20. LIMITATION OF ABSTRACT** UU

NSN 7540-01-280-5500 Standard Form 298 (Rev. 2-89) Prescribed by ANSI Std. 239-18

THIS PAGE INTENTIONALLY LEFT BLANK

Approved for public release. Distribution is unlimited.

SPECTRAL SHAPING AND SYMBOL ERROR MITIGATION TECHNIQUES TO INJECT OFDM SUBCARRIERS INTO NAVIGATIONAL RADAR GUARD BANDS AND MAINLOBE FOR SPECTRUM SHARING

Michelle L. Parmentar
Lieutenant, United States Navy
BS, University of Mary Washington, 2008

Submitted in partial fulfillment of the
requirements for the degree of

MASTER OF SCIENCE IN ELECTRICAL ENGINEERING

from the

NAVAL POSTGRADUATE SCHOOL
March 2019

Approved by: Ric Romero
Advisor

Tri T. Ha
Second Reader

Clark Robertson
Chair, Department of Electrical and Computer Engineering

THIS PAGE INTENTIONALLY LEFT BLANK

ABSTRACT

In this work, we investigate the effects of spectrally opportunistic shaped communications waveforms impinging into the spectrum of a radar. To simulate the radar, we first use a Hamming-based spectral shape and a more realistic spectrum from a commercial navigation (COMNAV) radar. The communications system employs orthogonal frequency-division multiplexing (OFDM) with the subcarriers modulated by quaternary phase-shift keying (QPSK). We utilize waterfilling, adhoc waterfilling inversion, and uniform energy distribution techniques to shape the communications spectrum, fill the spectral tails (i.e., guard bands), and even inject subcarriers into the radar bandwidth. Unsurprisingly, the high-powered radar interferes with the communications signal such that the symbol error ratio (SER) is drastically degraded. In addition to the spectral shaping techniques on transmit, we propose estimation and subtraction of the radar interference from the interfered subcarriers. The combination results in SERs that are vastly improved, while the radar probability of detection is minimally or slightly affected.

THIS PAGE INTENTIONALLY LEFT BLANK

Table of Contents

THIS PAGE INTENTIONALLY LEFT BLANK

List of Figures

List of Tables

THIS PAGE INTENTIONALLY LEFT BLANK

List of Acronyms and Abbreviations

AWGN	additive white Gaussian noise
AWI	adhoc waterfilling inversion
COMNAV	commercial navigation
CW	continuous wave
dB	decibel
DSSS	direct sequence spread spectrum
ESD	energy spectral density
FPGA	field programmable gate array
IF	intermediate frequency
ISI	inter-symbol interference
LPI	low probability of intercept
MDR	missed detection rate
MI	mutual information
MIMO	multiple-input, multiple-output
OFDM	orthogonal frequency-division multiplexing
PFA	probability of false alarm
PSD	power spectral density
QPSK	quaternary phase-shift keying
RCR	radar power-to-communications power ratio

RF radio frequency

RFI radio frequency interference

SER symbol error ratio

SNR signal-to-noise power ratio

UED uniform energy distribution

Acknowledgments

Thank you to my advisor, Dr. Romero. Without your patience and guidance, this thesis would not have been possible.

This thesis is dedicated to my parents.

THIS PAGE INTENTIONALLY LEFT BLANK

CHAPTER 1:
Introduction

Spectrum management is required to minimize radio frequency interference (RFI). Spectral isolation (e.g., the use of guard bands) is generally utilized to avoid signal interference between licensed users. With the growing number of devices requiring the use of the radio frequency (RF) spectrum, congestion mitigation is required. The idea of radar and communications operating within the same spectral band, instead of spectrally isolating the two applications, is a very active area of research.

Two applications for such joint radar-communications operations intend to maximize bandwidth usage. The first example application is motivated by the growing popularity of driver assistance in the automotive industry. The signals required to provide sensing for driver assistance must share the frequency spectrum with cellular communications signals. Similarly, unmanned or autonomous maritime vessels may utilize both radar and communications signals that require spectrum sharing. This type of spectrum sharing is reviewed in Section 1.1.

A second application of radar and communications operating within the same spectrum band is motivated by the need to hide information within the purview of another signal. The ability to disguise a weaker communications signal by transmitting it with a more powerful radar signal is discussed in Section 1.2. In this research work, we investigate the idea of radar and communications operating harmoniously within the same bandwidth.

1.1 Spectrum Sharing

When describing radar-communications spectrum sharing, the work in [1] proposed three system categories: coexistence, cooperation, and co-design. Coexistence, which is mostly applicable to spectrum sharing with legacy systems, assumes one system treats the second system as interference and requires mitigation. Cooperation implies the sharing of information between systems to mitigate interference. Co-design suggests the systems are designed jointly with the motivation of sharing spectrum space between them.

The work in [2] investigated a radar-communications fusion approach, where the author considered a joint radar-communications waveform for transportation applications. orthogonal frequency-division multiplexing and direct sequence spread spectrum were studied as options for a joint signal to provide radar sensing and communications. orthogonal frequency-division multiplexing (OFDM) yielded positive results within radar applications and direct sequence spread spectrum (DSSS) provided multi-user possibilities. The work in [3] designed a maritime multiple-input, multiple-output (MIMO) radar waveform to coexist with an existing cellular system. This design required knowledge of the communications channel as well as waveform design of a new system, i.e., the work took elements of all three system categories mentioned above. Similar to [3], the work in [4] examined the spectrum sharing between a radar and cellular system but focused on rotating radars (i.e., mechanical or electronic), and it specifically used examples of weather, air traffic control, and surveillance radars. The authors in [4] proposed transmitting the communications signal in its system's operational area when the radar's antenna beamwidth is pointed away to take advantage of the radar's rotational motion.

1.2 Covertness and LPI

Radar-embedded communications have been previously studied by [5] and recently in [6]-[8] with the motivation of potentially hiding a weaker communications signal in a radar waveform, such as in covert or low probability of intercept (LPI) communications. In [6]-[8], it was suggested to embed a low-power communications signal into a powerful radar signal coincident in time, resulting in the communications signal also occupying the radar's mainlobe and guard bands. The amount of overlap depends on how many symbols are embedded in one radar pulse. The works in [6]-[8] effectively assumed that the radar pulses are rectangular pulses, while the work in [9] proposed to use an approximated commercial navigation (COMNAV) radar waveform with spectral guard bands. For phase-coded continuous wave (CW) radar signals, a rectangualr pulse is assumed in each subpulse by [6]-[8]. Works in [6] and [7] examined the communications effect on radar's probability of detection P_D and symbol error ratio (SER) using quaternary phase-shift keying (QPSK) modulation, while the work in [8] examined additional M-ary modulation schemes.

Interestingly, the work in [10] employed a waterfilling method to spectrally shape a radar signal to occupy and exploit the nulls of the spectrum of a legacy QPSK communications

signal. The motivation of designing a radar waveform to fit in the null spaces of an existing communications system is similar to [3]. In this work, we completely reverse the problem in [10] by spectrally shaping the communications waveform to opportunistically exploit the guard bands (and even inject OFDM subcarriers) into the spectrum of a legacy commercial radar.

1.3 Objective

In this work, we completely deviate from the covert communications motivation of [6]-[8] and instead focus on exploitation of the radar guard bands (spectral tails) for spectral sharing, as in [2]-[3]. We start to encroach into the radar mainlobe as a way to increase the communications bandwidth. Inspired by the practical use of an approximated COMNAV radar pulse in [9], we diverge from the rectangular radar pulses considered in previous work by using practical pulse spectral shapes (e.g., Hamming or Taylor) and later use a more "practical" COMNAV radar waveform. We employ different spectral-shaping techniques based on the radar power spectral density (PSD) to form the magnitudes of the OFDM communications subcarriers. Exploiting the radar spectral tails while injecting extra subcarriers into the radar mainlobe enables increased communications throughput in an attempt to increase the communications bandwidth.

The first spectral technique we propose in designing the communications waveform is the waterfilling technique [11] which shapes the OFDM spectrum to take advantage of the frequencies where the radar is spectrally low. The second technique is an adhoc waterfilling inversion (AWI) method used by both radar PSDs where we individually code the subcarrier magnitudes in an adhoc fashion. By examining the missed detection rate (MDR) as a metric of performance, we show that both techniques have a minimal effect on the radar's P_D.

The work in [9] introduced a more realistic radar PSD based on COMNAV radar. In our simulations, we downsample this radar PSD to produce a radar spectrum which we denote in this work as "practical" COMNAV radar PSD. We employ different spectral shaping techniques to exploit the radar's spectrum to transmit OFDM communications subcarriers. We explore the waterfilling method, the adhoc technique which inverts the waterfilling method (which we call AWI), and finally we attempt to utilize the entire bandwidth and transmit through the radar mainlobe by distributing communications energy

uniformly across all subcarriers. As we recall the three radar-communications signal design categories in [1], we design an OFDM-based waveform based on prior knowledge of the radar PSD. This design can be placed in the "coexistence" category, since it integrates a new signal into the spectrum of a legacy signal and treats the legacy signal as interference. By using known radar parameters to estimate and subtract radar interference from the communications signal, we utilize both the 'coexistence" and "cooperation" categories.

We also differ from [6]-[9] by employing OFDM using QPSK for each subcarrier instead of simply using rectangular pulse-shaped QPSK modulation that fully encroached into the radar bandwidth; however, the spectral shaping techniques can only modestly improve SER. Assuming the radar signal is more powerful than the communications signal, the injected subcarriers will be interfered by the legacy radar waveform regardless of spectral shaping. Estimation and subtraction of the radar's interference greatly improve the SER depending on the number of received symbols in which to perform the estimate.

1.4 Thesis Organization

In Chapter 2, we begin by describing our radar and communications signal models. Further, we investigate spectral-shaping techniques for OFDM subcarriers to utilize guard bands and inject subcarriers into radar bandwidth. In Chapter 3, we explore demodulation of the communications signal and attempt to correct the radar waveform interference by using estimation and subtraction. In Chapter 4, we evaluate the communications' SER and the radar's percentage or probability of detection P_D. Finally, in Chapter 5, we summarize our conclusions and recommend follow-on work.

CHAPTER 2:
Signal Models

As is customary in signal processing, we employ a complex-valued baseband signal model at the radar and communications receivers. We assume normalized sampling time with $T_s = 1$. The discretized signal, either in the radar receiver or communications receiver, can be modeled by

$$y[n] = r[n] + c[n] + w[n], \tag{2.1}$$

where $r[n]$ is the radar signal, $c[n]$ is the communications signal, $w[n]$ is zero mean complex-valued additive white Gaussian noise (AWGN) with noise variance σ^2, and $n = 0, 1, 2, 3, ..., N_n - 1$. When evaluating P_D, the communications waveform acts as interference on the radar. Conversely, when evaluating SER, the radar acts as interference on the communications system.

2.1 Radar

We model the radar signal $r[n]$ using two different power spectral densities. We start our analysis using a Hamming-based PSD and further examine the simulations using a more practical downsampled COMNAV radar PSD described in Section 2.1.1-2.1.2, respectively.

2.1.1 Hamming-Based PSD

We model the radar signal $r[n]$ using Hamming-based radar PSD, which is more realistic than the sinc-shaped spectrum assumed in [6]-[8] and is shown in Figure 2.1 (a). The width of the guard bands depend on how stringent the radar requirements are. For example, a loose requirement of -13 dBc (decibel (dB) from center frequency) will place the guard bands at approximately $|f| > 0.35$ in Figure 2.1 (a). The radar power-to-communications power ratio (RCR) is defined as P_r/P_c where P_r is the radar power and P_c is the communications power.

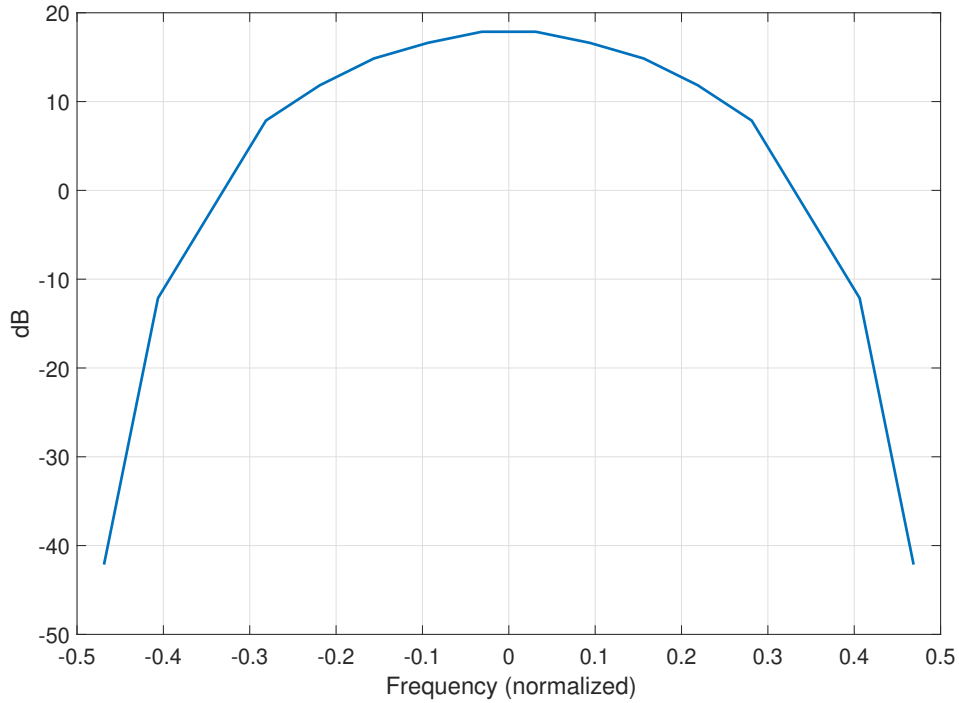

(a) Hamming-based radar PSD.

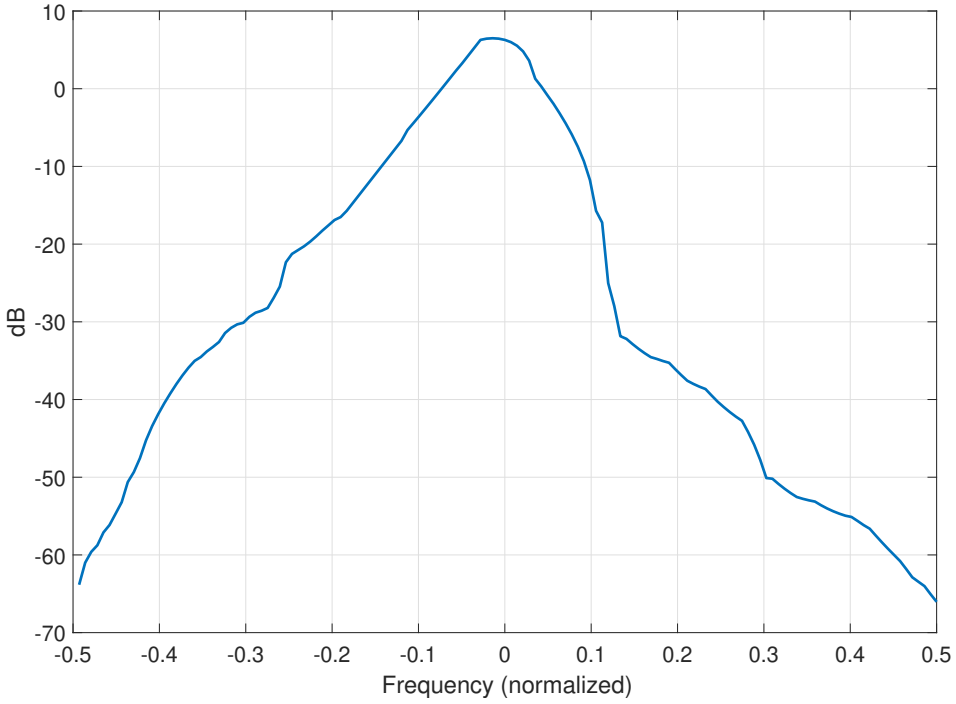

(b) Practical COMNAV radar PSD.

Figure 2.1. Radar PSDs used for simulations.

2.1.2 Practical COMNAV Radar PSD

We model the radar signal $r[n]$ using a more realistic but an approximate COMNAV radar spectrum [9] as shown in Figure 2.1 (b). For simulation purposes, we downsample the PSD to 16 samples while still approximating the spectral tails that occupy the radar guard bands. The choice of 16 frequency bins represents 16 subcarriers that we will use for our simulations.

2.2 Communications Signal

To utilize the radar guard bands, it is intuitive to place all the OFDM subcarriers on the spectral tails of the radar having almost zero overlap as shown in Figure 2.2 (a). The subcarriers (slots) are represented by the "red stems or dots" and are numbered sequentially from left to right (potential subcarriers 1-16). Due to practically zero overlap between the utilized OFDM subcarriers (subcarriers 1-3 and 14-16) and the radar spectrum (i.e., where the radar power is low) and the intuitive placement of OFDM subcarriers, SER approaches that of the theoretical QPSK SER. To increase throughput (without going into higher order M-ary modulation) beyond the guard bands, we ambitiously propose to inject more subcarriers in the radar mainlobe knowing that SER will be greatly degraded. The question becomes "how far into the radar mainlobe can we inject subcarriers with acceptable SER?"

2.2.1 Frequency Domain Waterfilling

We first explore the waterfilling technique described in [10]-[11]. In our application, the design of the communications waveform is dependent upon the radar and noise interference. According to [11], we see that maximizing mutual information (MI) (and, thus, capacity) yields the energy spectral density (ESD) of the waveform desired, given by

$$\left|X[f]\right|^2 = \max\left[0, A - \frac{S_{nn}[f]}{\lambda[f]}\right], \tag{2.2}$$

where A is a parameter to be searched during optimization and $\lambda[f]$ is the desired communications ESD if the interference were purely AWGN. In other words, the ideal $\lambda[f]$ spectrum would not be partial to any subcarrier if the interference is spectrally flat. Indeed, in the case of AWGN-only interference, the thermal noise is considered to have equal power at all frequencies and, thus, $\lambda[f]$ is also constant for all frequencies. The communications'

energy constraint is given by

$$E_x - \frac{\delta}{2} \leq \int_W \left|X[f]\right|^2 df \leq E_x + \frac{\delta}{2} \tag{2.3}$$

where δ is is the error tolerance desired, W is the signal bandwidth, and $\frac{S_{nn}[f]}{\lambda[f]}$ is the function to be waterfilled. The total interference PSD is given by

$$S_{nn}[f] = P_r[f] + P_n[f], \tag{2.4}$$

which is the summation of the radar PSD $P_r[f]$ and noise PSD $P_n[f]$. When the communications energy is small, the result of the frequency-domain waterfilling is to simply use the spectral tails of the radar, which is intuitive, but is the trivial solution discussed above, where the waterfilled communications spectrum does not overlap with the radar mainlobe and vice versa. As expected, the SER closely follows the QPSK theoretical SER, given by [13]

$$P_E = 2Q\left(\sqrt{\frac{E_s}{N_0}}\right) \tag{2.5}$$

where E_s denotes the symbol energy and N_0 denotes the noise PSD. By using a medium energy constraint for the waterfilling algorithm, we see that the communications waveform starts to encroach into the radar spectrum.

The waterfilling spectral shaping technique utilizing the Hamming-based radar PSD is shown in Figure 2.2 (b). At RCR = 0 dB and communications signal-to-noise power ratio (SNR) at 13 dB, the waterfilling method assigns 12 subcarriers, with subcarriers 6 and 11 being fully interfered by the radar mainlobe. We see in Figure 2.3 (a) that the waterfilling technique assigns 14 subcarriers when using the practical radar PSD. As the energy constraint increases, the communications waveform intrudes further into the radar mainlobe. Such action results in significant radar interference in the subcarriers injected in the radar mainlobe and is examined in Chapter 3.

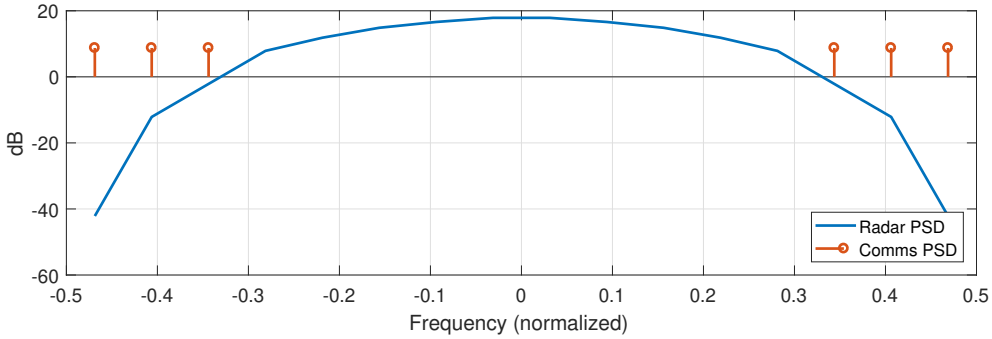

(a) Almost zero spectral overlap.

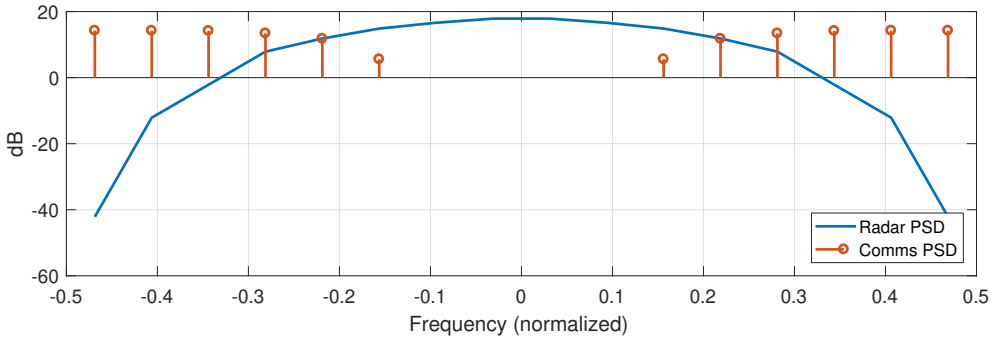

(b) Waterfilled spectral shaping technique.

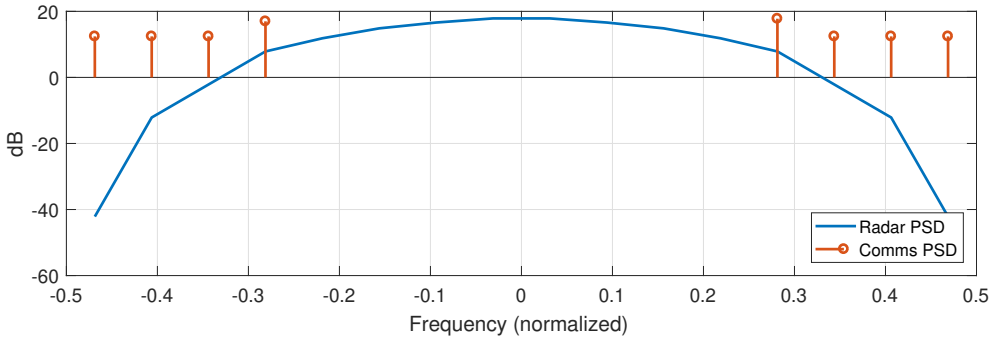

(c) AWI spectral shaping technique.

Figure 2.2. Radar with Hamming-based PSD radar spectrum with spectrally shaped communications waveform using QPSK modulated subcarriers at RCR = 0 dB and SNR = 13 dB.

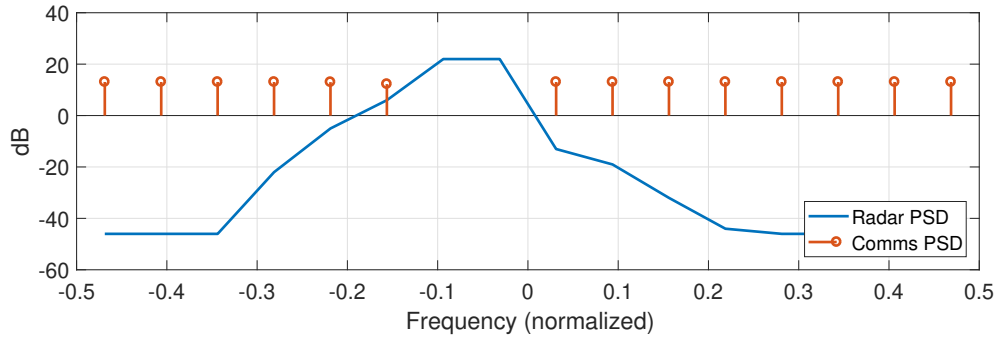

(a) Waterfilling spectral shaping technique.

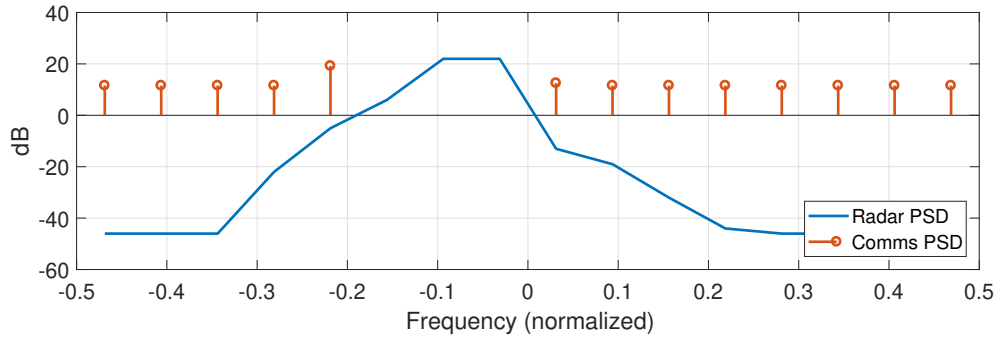

(b) AWI spectral shaping technique.

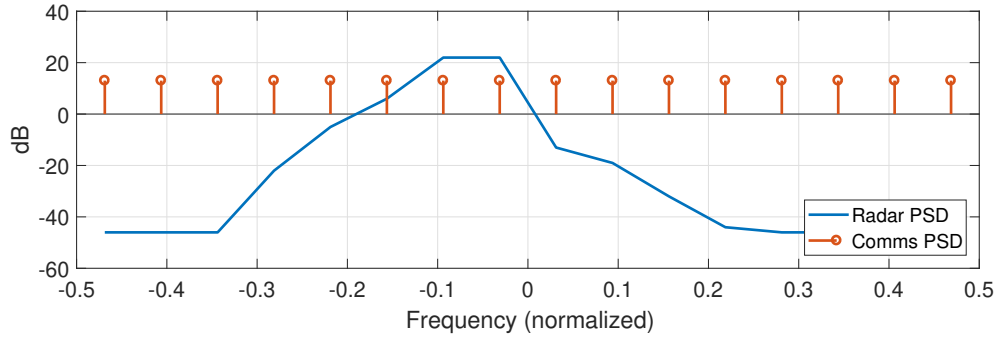

(c) UED spectral shaping technique.

Figure 2.3. Practical COMNAV radar PSD with spectrally shaped communications waveform using QPSK modulated subcarriers at RCR = 0 dB and SNR = 13 dB.

2.2.2 AWI for Hamming-Based Radar PSD

When the communications' energy is large enough (i.e., RCR is low), the waterfilling method injects some subcarriers in the radar mainlobe in an effort to take advantage of the

lowered radar power. Unfortunately, this action drastically degrades SER. We found to a degree that the AWI method is sometimes successful. In this technique, we assign the subcarrier magnitudes such that the subcarriers which intersect with the radar mainlobe receive more energy than the ones on the spectral tails to offset the symbol errors from the radar interference. The subcarriers on the spectral tails receive less energy such that there is some increase in symbol errors. This type of assignment of subcarrier magnitudes is clearly the opposite of the waterfilling technique, which is why the technique is called the adhoc waterfilling inversion method. We illustrate the AWI method in Figure 2.2 (c) with eight subcarriers at RCR = 0 dB and SNR = 13 dB. Subcarriers 4 and 13 receive more energy than the ones on the spectral tails.

2.2.3 AWI for Practical Radar PSD

The AWI technique for our practical COMNAV radar PSD is similar to Section 2.2.2 in that we assign the subcarrier magnitudes such that the subcarriers which intersect with the radar mainlobe receive more energy than the ones on the spectral tails to offset the symbol errors from the radar interference. We illustrate the AWI method for the practical COMNAV radar PSD in Figure 2.3 (b) at RCR = 0 dB and SNR = 13 dB, which yields 13 QPSK subcarriers.

2.2.4 Uniform Energy Distribution across All Subcarriers

We continue our effort to increase throughput beyond the guard bands and utilize all available subcarriers slots. Contrary to assigning subcarrier magnitudes which intersect with the radar mainlobe with higher energy for AWI and algorithmically assigning subcarrier magnitudes with waterfilling, we assign uniform energy to all subcarriers, hence the name UED. As shown in Figure 2.3 (c), subcarriers 7-8 are completely enveloped by the radar mainlobe. UED using the Hamming-based radar is similar to Figure 2.3 (c), with subcarriers occupying the entirety of the bandwidth. Injecting communications subcarriers into the radar mainlobe will certainly have an adverse affect on the radar probability of detection, which we explore in Chapter 4.

2.3 Signal Block Diagram for Simulations

The overall signal block diagram for simulations is depicted in Figure 2.4. As mentioned, we utilize two radar spectral models in this work; thus, we switch between the radar PSDs in

our simulations to use for spectrally shaping the communications waveform. We also utilize three different spectral shaping techniques and modulate each resulting OFDM subcarrier with QPSK modulation. The communications signal experiences interference from the radar signal depending on its power and the AWGN from the receiver.

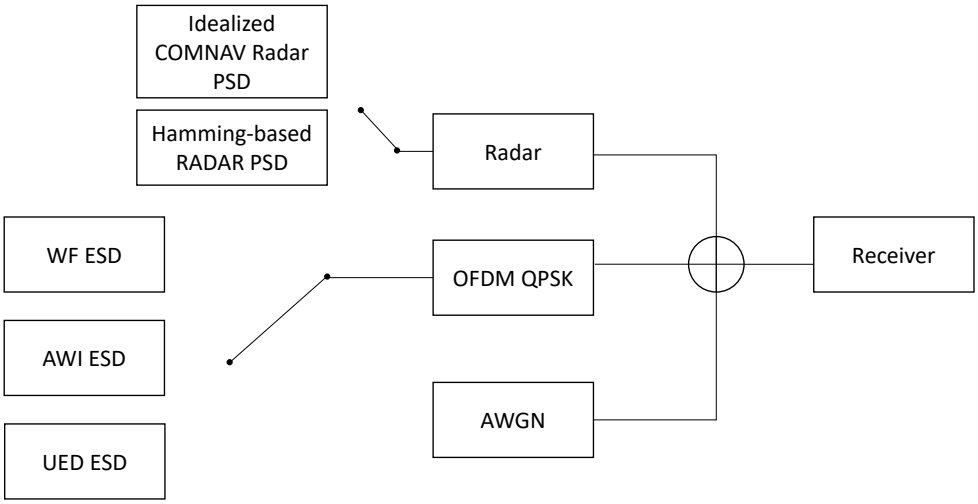

Figure 2.4. Signal block diagram for simulations.

CHAPTER 3:
Downconversion and Demodulation Techniques

First, we examine the case where downconversion and demodulation of the communications signal are performed. As shown in Figure 3.1, the communications signal is received at the antenna, is downconverted from RF to an intermediate frequency (IF), and passes through an IF notch filter. The communications receiver assumes the knowledge of radar PSD and eliminates portions of the radar energy where the communications signal is spectrally absent, i.e., the radar mainlobe. The communications receiver does not assume knowledge of the phase or magnitude of the radar waveform and interference remains in the subcarriers where the radar energy is spectrally low. After passing through the notch filter, the QPSK subcarriers are demodulated.

3.1 Signal Constellation and SERs with Waterfilling and AWI Spectral Shaping

We examine signal constellations and SERs for each spectral shaping technique for both the Hamming-based radar and practical radar PSDs. We see in each case that communications performance is limited due to the radar interference.

3.1.1 Waterfilling, AWI, and UED with Hamming-Based Radar PSD

Signal spaces for waterfilling, AWI, and UED communications spectral techniques applied to the Hamming-based radar PSD are presented in this section using Monte Carlo simulations of 10^6 trials.

3.1.1.1 Signal Constellation Using Waterfilling Method

The QPSK signal spaces for six waterfilled subcarriers simulated at RCR = 10 dB and SNR = 13 dB are shown in Figure 3.2. Notice that the radar interference causes an amplitude/phase shift in subcarriers 3 and 14. In this work, we arbitrarily used an amplitude shift with 0 degree phase shift for illustration (but any phase shift can be accommodated in our methods and simulations).

3.1.1.2 Signal Constellation Using AWI Method

Similarly, we have the QPSK signal spaces with AWI subcarriers simulated at RCR = 10 dB and SNR = 13 dB in Figure 3.3. Notice that eight subcarriers are used, and the innermost subcarriers 4 and 13 yield significant errors. It will be shown that while the AWI method may work well in some cases, just like the waterfilling method, it is not able to fully correct the constellation shift due to radar interference in the injected subcarriers.

3.1.1.3 Signal Constellation Using UED Method

Finally, we have the QPSK signal spaces with UED subcarriers simulated at RCR = 10 dB and SNR = 13 dB in Figure 3.4. Notice that 16 subcarriers are used, and the innermost subcarriers 8-9 yield substantial errors. It will be shown that the UED method provides the most symbol errors of the three techniques utilized.

3.1.2 SERs for Waterfilling, AWI, and UED Techniques Using Hamming-Based Radar

The corresponding SERs for the waterfilling technique, AWI, and UED techniques are shown for RCR = 10 dB in Figure 3.5. The waterfilling and AWI techniques provide moderate improvement over the UED method; however, these three methods do not approach the theoretical QPSK SER, which motivates us to investigate other scenarios where any of these techniques may work well.

3.1.3 Signal Constellations Using Practical COMNAV Radar PSD

Due to the lower spectral tails of the practical COMNAV radar PSD, we are able to include more subcarriers in our spectral shaping technique compared to the Hamming-based radar. Signal spaces for waterfilling, AWI, and UED communications spectral techniques which are applied to a practical COMNAV radar PSD are presented in this section. We expect to see the most radar interference in the UED subcarriers that are engulfed by the radar mainlobe.

3.1.3.1 Signal Constellation Using Waterfilling Method

The QPSK signal constellation resulting from the waterfilling technique is shown in Figure 3.6 at RCR = 10 dB and SNR = 13 dB. At RCR = 10 dB, the waterfilling method

assigns 13 subcarriers. A constellation shift is apparent in subcarriers 4-5 as well as slight shifts in subcarriers 9 and 10.

3.1.3.2 Signal Constellation Using AWI Spectral Shaping Method

An example constellation for the AWI technique is shown in Figure 3.7 at RCR = 10 dB and SNR = 13 dB. The AWI technique for the practical COMNAV radar PSD uses 13 subcarriers, and the subcarriers within the radar mainlobe (subcarriers 4, 5, and 9) contain symbol errors. This is evident in the constellation shifts.

3.1.3.3 Signal Constellation Using UED Spectral Shaping Method

We use all 16 subcarriers with uniform energy distribution in our final example, as shown in Figure 3.8. From the signal spaces, we see constellation shifts in subcarriers 4-10, significant errors in subcarriers 7 and 8, moderate errors in subcarriers 5-6, and very slight radar interference in subcarriers 4, 9, and 10.

3.1.4 SERs Using Practical COMNAV Radar PSD

The SERs for the waterfilling, AWI, and UED techniques are depicted in Figure 3.9 for RCR = 10 dB. As expected, the UED technique experiences the most radar interference, and subsequently, its SER is the least desirable. The AWI technique approaches the theoretical QPSK SER most closely compared to the other two techniques. This adhoc but careful choice of energy allocation clearly works well to mitigate radar interference in this scenario. The three techniques may work well in some cases, but they are not able to fully correct the constellation shifts due to radar interference in the injected subcarriers. In Figure 3.10, we see all the SERs for all the spectral shaping techniques at RCR = 10 dB. The question becomes, while we introduced transmit-centric spectral techniques, is there a receive-centric technique to correct the phase/amplitude shifts in the interfered subcarriers? If so, can we achieve better performance while maintaining throughput for some of these techniques? For the former question, a correction method is introduced in Section 3.2. For the latter, we present extensive analyses of various scenarios involving SER and throughput trade offs in 4.1.3.

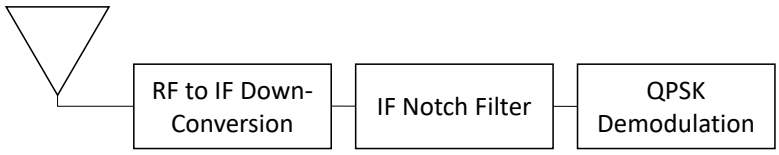

Figure 3.1. Received signal block diagram including RF downconversion, IF filtering, and QPSK demodulation of the radar-interfered communications signal.

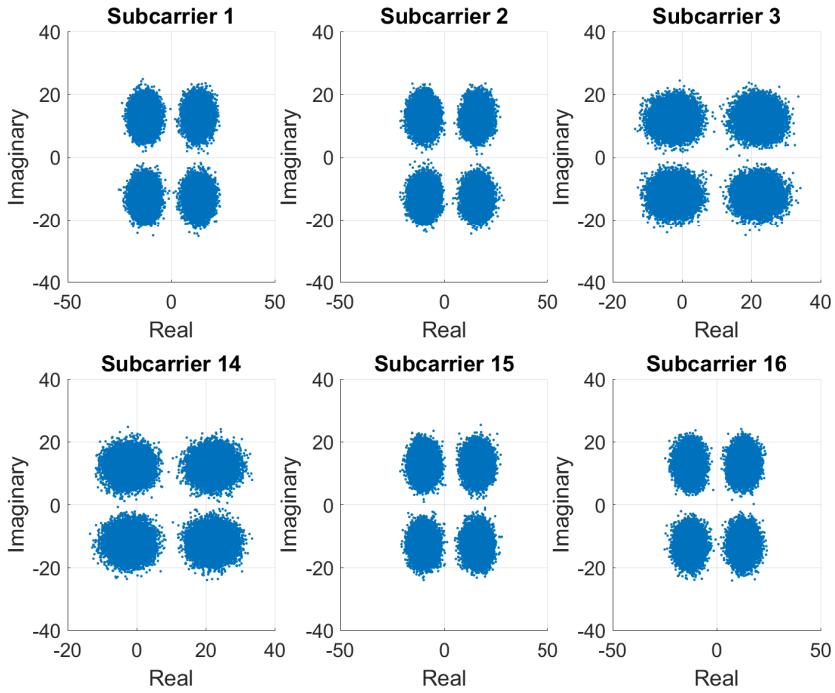

Figure 3.2. QPSK signal spaces with six waterfilled subcarriers simulated at RCR = 10 dB and SNR = 13 dB. Radar interference causes a shift in subcarriers 3 and 14.

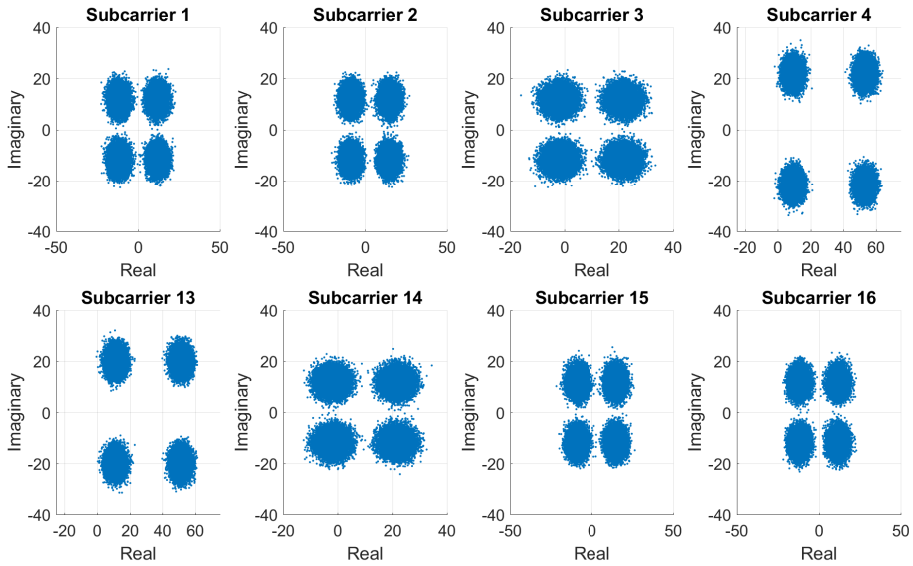

Figure 3.3. QPSK signal spaces with eight AWI subcarriers simulated at RCR = 10 dB and SNR = 13 dB. Radar interference causes a phase/amplitude shift in subcarriers 3, 4, 13, and 14.

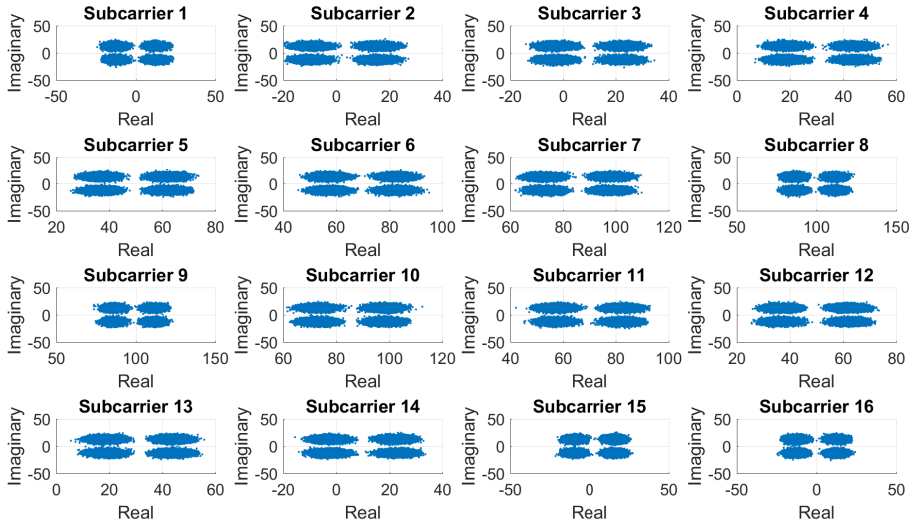

Figure 3.4. QPSK signal space with 16 UED subcarriers simulated at RCR = 10 dB and SNR = 13 dB. Radar interference causes a phase/amplitude shift in subcarriers 2-15.

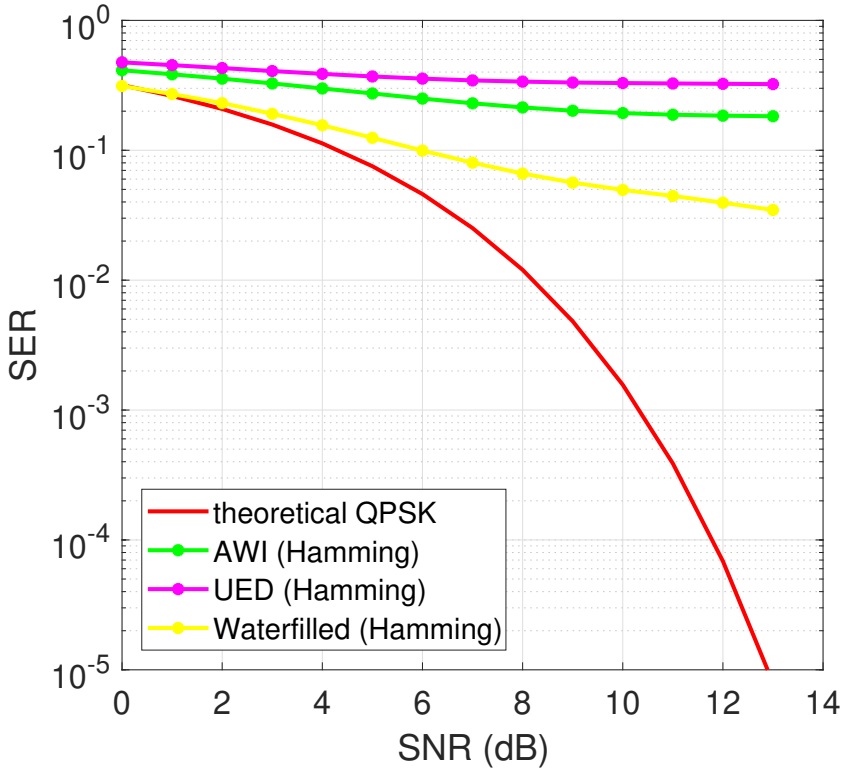

Figure 3.5. SER for waterfilled, AWI, and UED techniques at RCR = 10 dB.

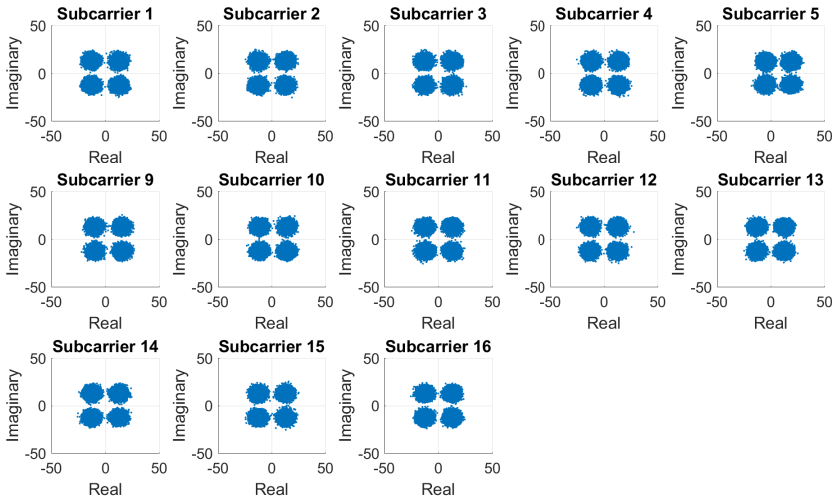

Figure 3.6. QPSK signal spaces with 13 waterfilled subcarriers simulated at RCR = 10 dB and SNR = 13 dB. Radar interference causes a phase/amplitude shift in subcarriers 4-5, 9, and 10.

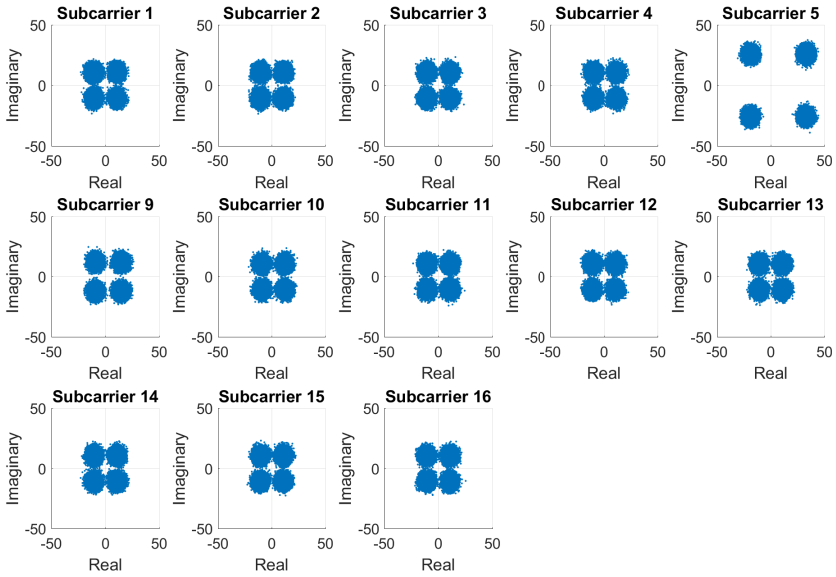

Figure 3.7. QPSK signal spaces with 13 AWI subcarriers simulated at RCR = 10 dB and SNR = 13 dB. Radar interference causes a phase/amplitude shift in subcarriers 4-5, and 9.

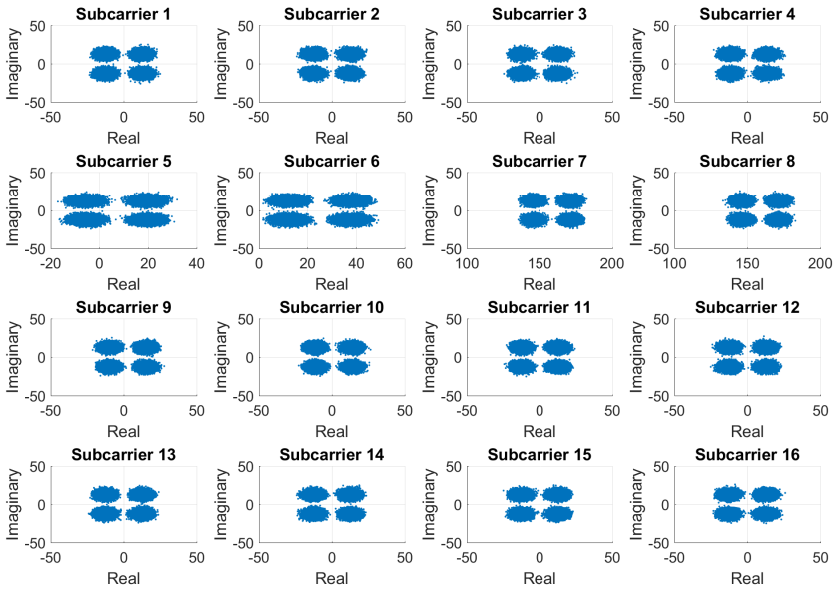

Figure 3.8. QPSK signal space with 16 UED subcarriers simulated at RCR = 10 dB and SNR = 13 dB. Radar interference causes a phase/amplitude shift in subcarriers 4-10.

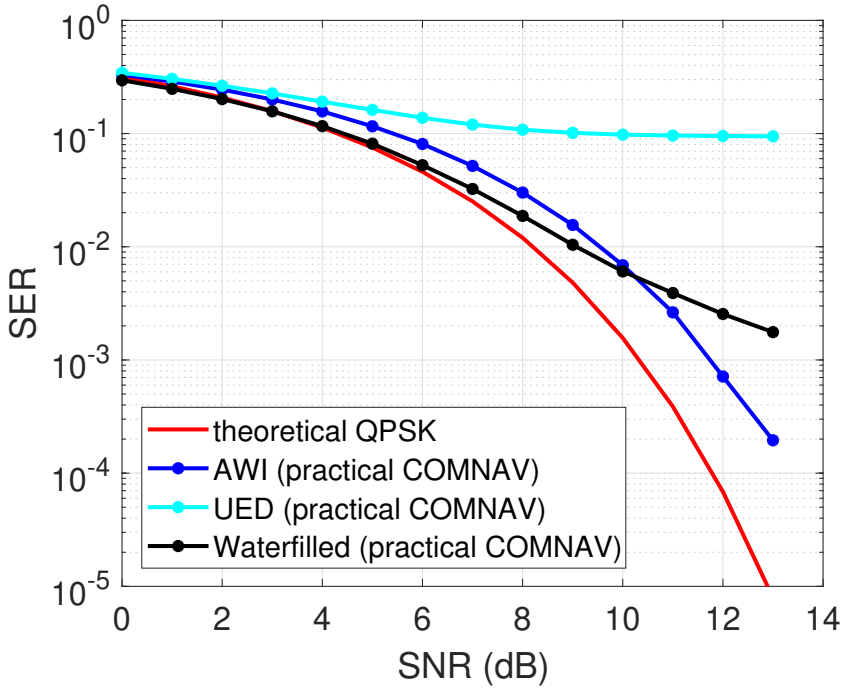

Figure 3.9. SER for AWI, UED, and waterfilling techniques calculated at RCR = 10 dB.

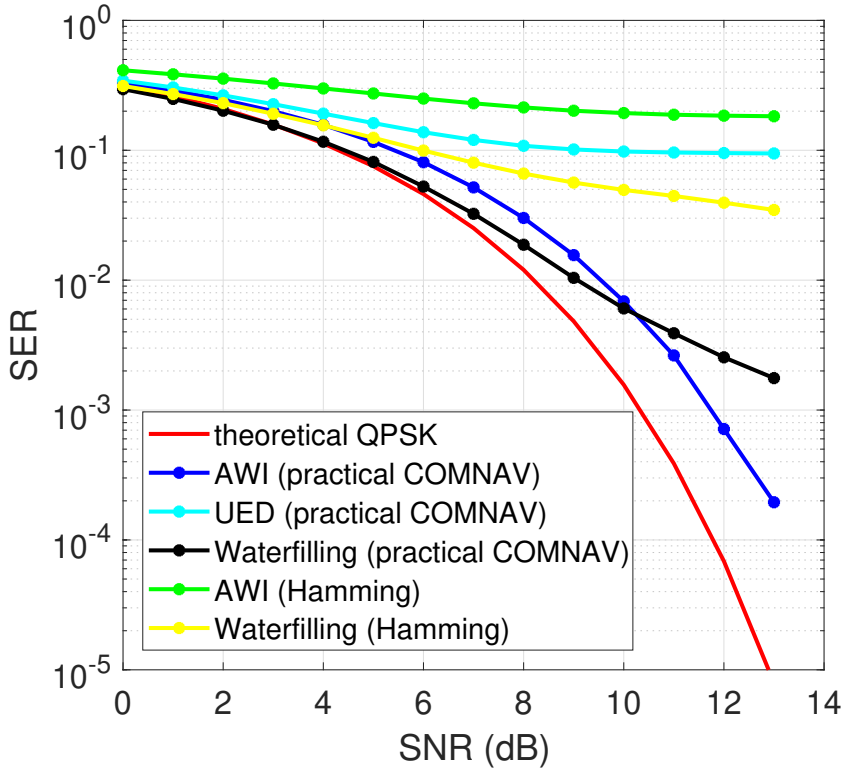

Figure 3.10. SER for AWI, UED, waterfilling (practical COMNAV radar PSD), AWI and waterfilling (Hamming-based radar PSD) techniques calculated at RCR = 10 dB.

3.2 Radar Interference Estimation and Subtraction

As shown above, purely spectral waterfilling and AWI techniques can only improve the SER modestly and in some cases do not work well. The subcarriers injected into the radar mainlobe will always experience radar interference, which translates into symbol errors in the receiver. From the previous constellation diagrams, we observe that rather than purely mitigating the problem in the waveform transmission by spectrally manipulating the magnitude of the injected subcarriers, we can make the correction in the receiver on top of spectral shaping. While the communications receiver assumes the knowledge of radar PSD, it does not assume knowledge of the phase or magnitude (i.e., the complex-valued amplitude) of the actual time waveform. Indeed, this is usually what happens in practice; however, it is also clear that only the injected carriers are interfered and an estimate of the complex-valued amplitude of the interfered subcarrier may be performed. Any technique

requires some subcarrier symbols to be received prior to estimation in order for subtraction to proceed.

First, we consider the case where a substantially large number of symbols are received per interfered carrier, i.e., latency is not an issue. This could be an example of a large data download. For both the waterfilling and AWI techniques, we estimate the mean of each subcarrier and subtract it from the received symbols, forming effectively near zero-mean and corrected subcarriers. Using such a large number of symbols is not practical for various practical applications (e.g., voice communications or any other real-time application).

As such, we propose to collect a finite number of symbols from each interfered subcarrier, perform the mean estimation, and then subtract the mean estimate to complete the correction. In our Monte Carlo simulations, we performed the correction using $N = 2^5, 2^6, 2^7$, and 2^8 symbols from the corresponding subcarrier. This method differs greatly from the approach in [6] in that the unknown phase and magnitude of the radar has to be corrected and subtracted from the whole received signal. Here, the interference magnitude and phase may be different from subcarrier to subcarrier. Our modified received RF-to-baseband signal block diagram is shown in Figure 3.11.

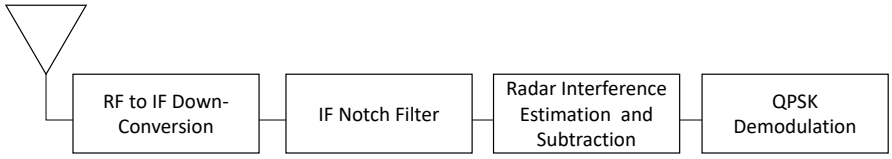

Figure 3.11. Received RF-to-baseband signal block diagram radar interference correction.

3.3 Spectrum Sharing and Demodulation Correction

We now apply the mean estimation and subtraction to all spectral shaping techniques prior to demodulation. We see in Figures 3.12-3.17 that the radar interference phase/amplitude shifts have been corrected for all frequency methods. This enables effective spectrum sharing between the communications and radar signals.

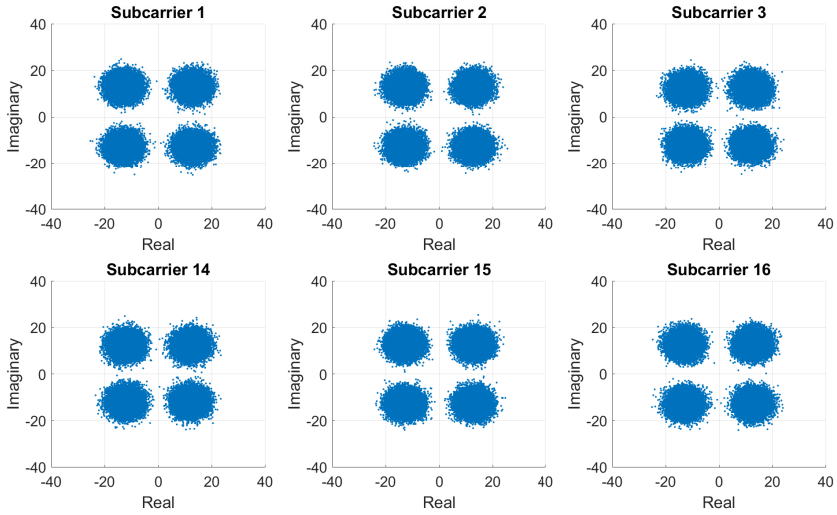

Figure 3.12. Subcarrier QPSK signal spaces with waterfilling technique after applying estimation corrections, which are simulated at RCR = 10 dB and SNR = 13 dB. Radar interference is corrected in the affected subcarriers.

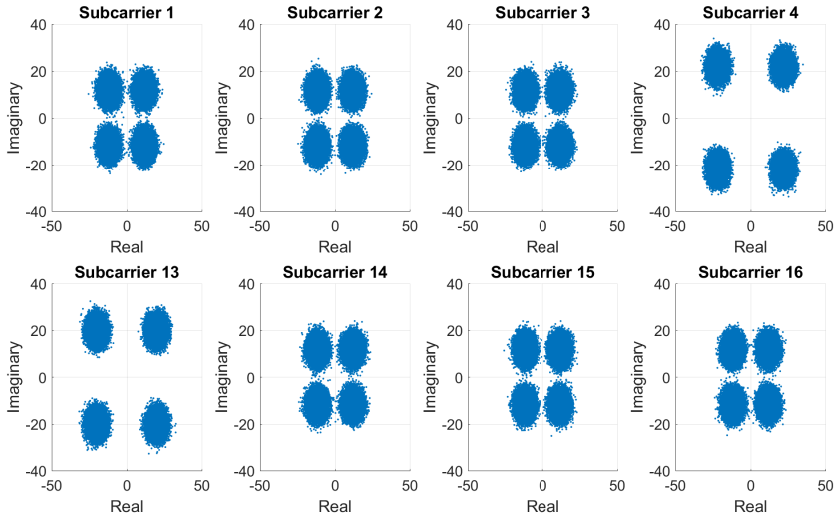

Figure 3.13. Subcarrier QPSK signal spaces with AWI technique space after applying estimation corrections, which are simulated at RCR = 10 dB and SNR = 13 dB. Radar interference is corrected in the affected subcarriers.

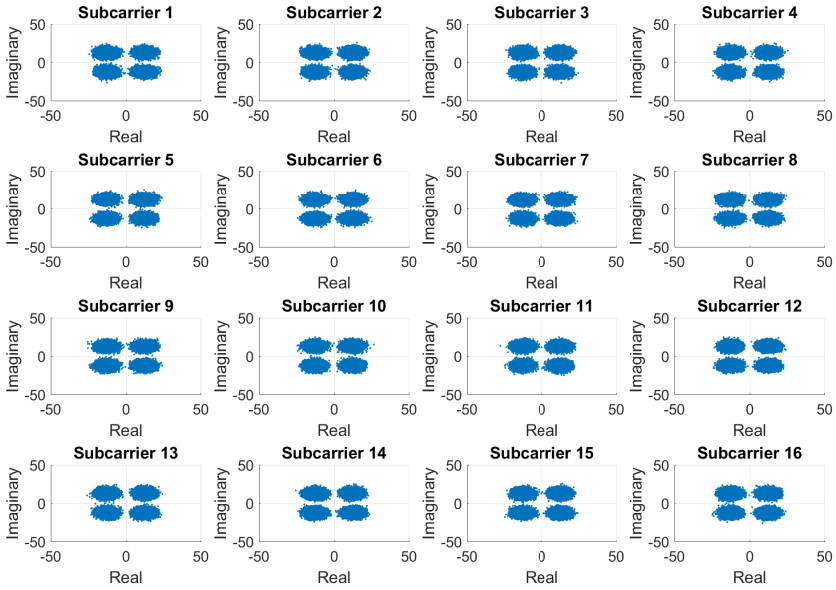

Figure 3.14. Subcarrier QPSK signal spaces with UED technique space after applying estimation corrections, which are simulated at RCR = 10 dB and SNR = 13 dB. Radar interference is corrected in the affected subcarriers.

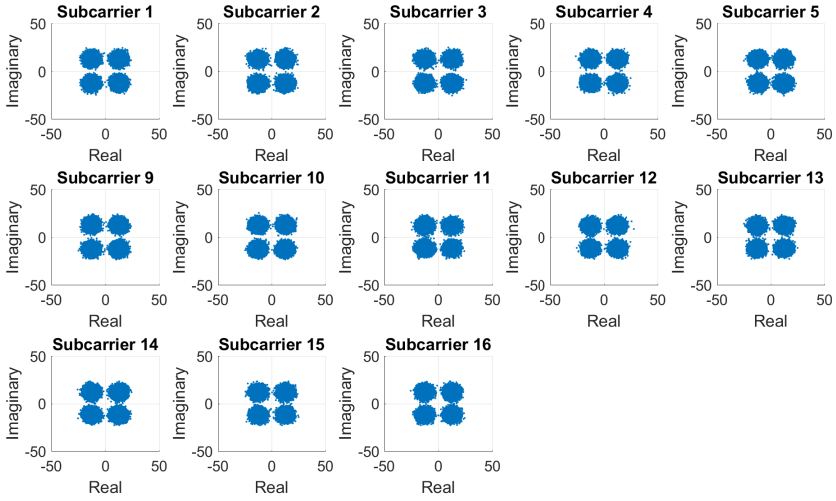

Figure 3.15. Subcarrier QPSK signal spaces with waterfilling technique using practical COMNAV radar PSD after applying estimation corrections, which are simulated at RCR = 10 dB and SNR = 13 dB. Radar interference is corrected in the affected subcarriers.

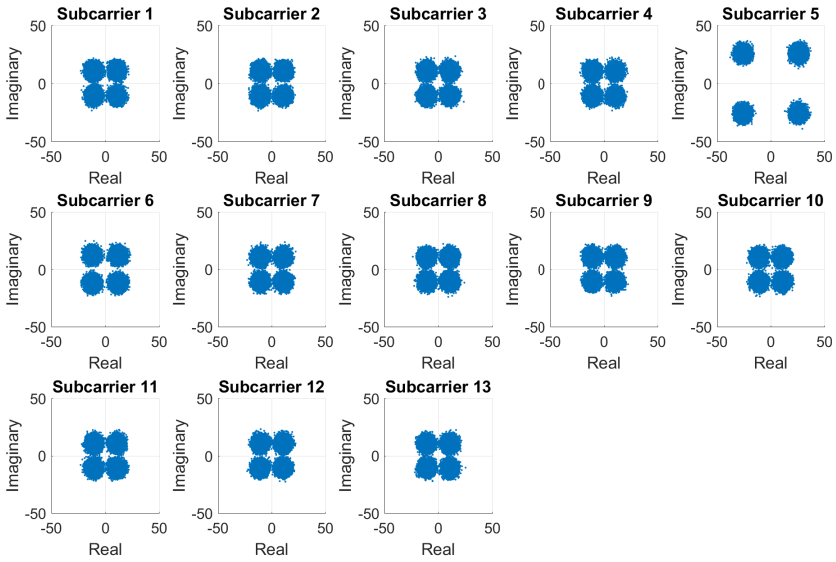

Figure 3.16. Subcarrier QPSK signal spaces with AWI technique using practical COMNAV radar PSD after applying estimation corrections, which are simulated at RCR = 10 dB and SNR = 13 dB. Radar interference is corrected in the affected subcarriers.

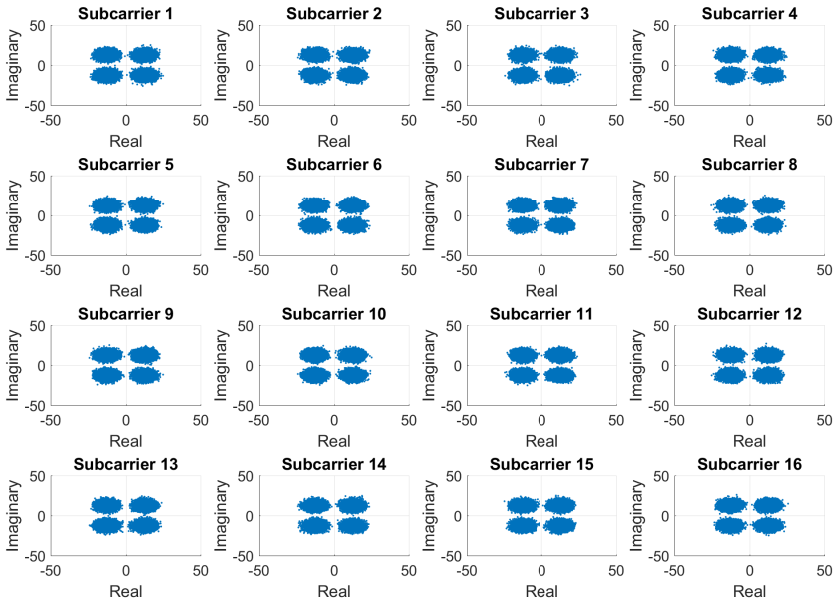

Figure 3.17. Subcarrier QPSK signal spaces with UED technique using practical COMNAV radar PSD after applying estimation corrections, which are simulated at RCR = 10 dB and SNR = 13 dB. Radar interference is corrected in the affected subcarriers.

THIS PAGE INTENTIONALLY LEFT BLANK

CHAPTER 4:
Results

4.1 SER

In the following sections, we examine the SERs for the spectral techniques associated with the Hamming-based radar PSD and the practical COMNAV radar PSD. We analyze the performance of waterfilling and AWI methods designed for the Hamming-based radar PSD and identify the scenarios with the most desirable SER in Section 4.1.1. In Section 4.1.2 we analyze the waterfilling, AWI, and UED methods designed for the practical radar PSD. Additionally, we compare the waterfilling and AWI methods and identify the best SER for each RCR regardless of throughput and then identify the best SER for each RCR while prioritizing throughput. We conclude Section 4.1.2 by comparing all three spectral shaping techniques utilizing the practical radar PSD by identifying the best SER for each N. In Section 4.1.3, we compare all five techniques utilizing both radar PSDs and identify the best SER for each N.

4.1.1 Using Hamming-Based Radar PSD

For the Hamming-based radar PSD, we examine the SERs after estimating and subtracting radar interference from the waterfilling and AWI communications spectral shaping techniques.

4.1.1.1 Using Waterfilling with Correction

At RCR = 20 dB, the waterfilling method, which utilizes six subcarriers, does not approach the theoretical SER at high values of N, as seen in Figure 4.1 (a). In this case, the radar power is too large. At RCR = 10 dB, the waterfilling method, which also utilizes six subcarriers, most closely approaches the theoretical SER for increasing values of N, as seen in Figure 4.1 (b). Intuitively, RCR = 5 dB should report the best SER performance (if waterfilling does not add extra subcarriers); however, waterfilling is designed to maximize the MI (i.e., it tries to increase throughput but does not minimize SER) by assigning eight subcarriers, which unfortunately sacrifices SER as shown in Figure 4.1 (c). At RCR = 10 dB, the waterfilling

method utilizes only six subcarriers, decreasing throughput while achieving better SER over RCR = 5 dB. A list involving RCR, number of subcarriers, and SER corresponding to N symbols collected for correction is given in Table 4.1, with $N = 0$ denoting the uncorrected case.

Table 4.1. SER performance for waterfilling based on RCR, number of subcarriers, and N symbols collected for correction.

RCR (dB)	Number of Subcarriers	SER at $N = 0$	SER at $N = 32$	SER at $N = 256$
0	12	1.7×10^{-1}	1.2×10^{-2}	9.8×10^{-3}
5	8	1.2×10^{-1}	1.8×10^{-3}	1.1×10^{-4}
10	6	3.5×10^{-2}	8.4×10^{-5}	1.5×10^{-5}
20	6	1.7×10^{-1}	1.5×10^{-2}	6.7×10^{-3}

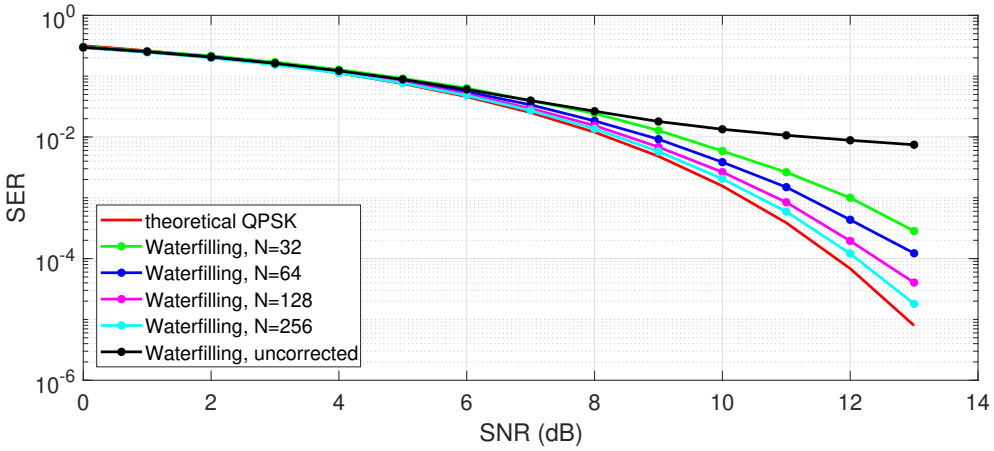

(a) RCR = 20 dB

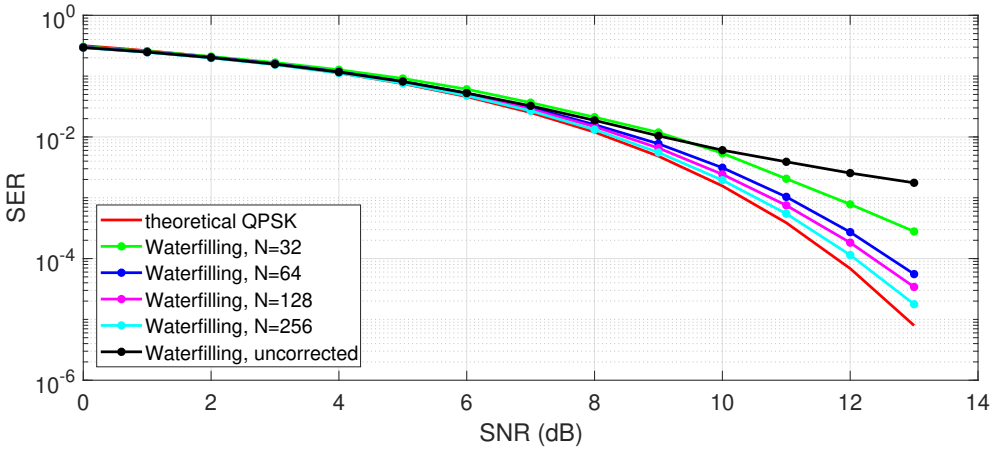

(b) RCR = 10 dB

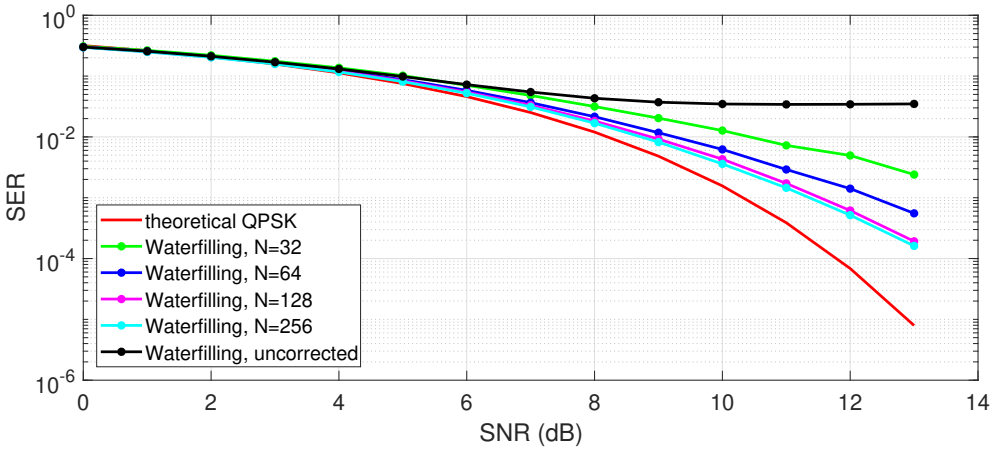

(c) RCR = 5 dB

Figure 4.1. SER vs. SNR (E_s/N_o) with waterfilling technique for various RCR values.

4.1.1.2 Using AWI with Correction

To increase throughput, we design the AWI method to maintain eight subcarriers despite increasing RCRs. At RCR = 20 dB, the AWI method performs well for all values of N. The AWI method has the closest SER to theoretical with $N = 256$ at RCR = 20 dB as seen in Figure 4.2 (a). At RCR = 10 dB, the AWI technique unsurprisingly has inferior performance compared to the waterfilling technique at RCR = 10 dB. This is due to the fact that we continue to use eight subcarriers for the AWI method, while the waterfilling technique utilizes six subcarriers (thus, less interference), as seen in Figure 4.2 (b). At RCR = 5 dB and RCR = 20 dB, the corrected AWI method performs better than the waterfilling method. At RCR = 5 dB, the AWI method performs better at $N = 32$ compared to waterfilling; however, the AWI and waterfilling method have similar performance at $N = 256$, as seen in Figure 4.2 (c). A list involving RCR, number of subcarriers, and SER corresponding to N symbols collected for correction is given in is given in Table 4.2, with $N = 0$ denoting the uncorrected case.

Table 4.2. SER performance for AWI communications comparing RCR, number of subcarriers, and N symbols collected for correction.

RCR (dB)	Number of Subcarriers	SER at $N = 0$	SER at $N = 32$	SER at $N = 256$
0	8	1.2×10^{-4}	1.5×10^{-4}	2.6×10^{-5}
5	8	1.7×10^{-2}	2.4×10^{-4}	3.5×10^{-5}
10	8	1.5×10^{-1}	1.1×10^{-3}	3.5×10^{-4}
20	8	2.8×10^{-1}	7.1×10^{-5}	4.6×10^{-5}

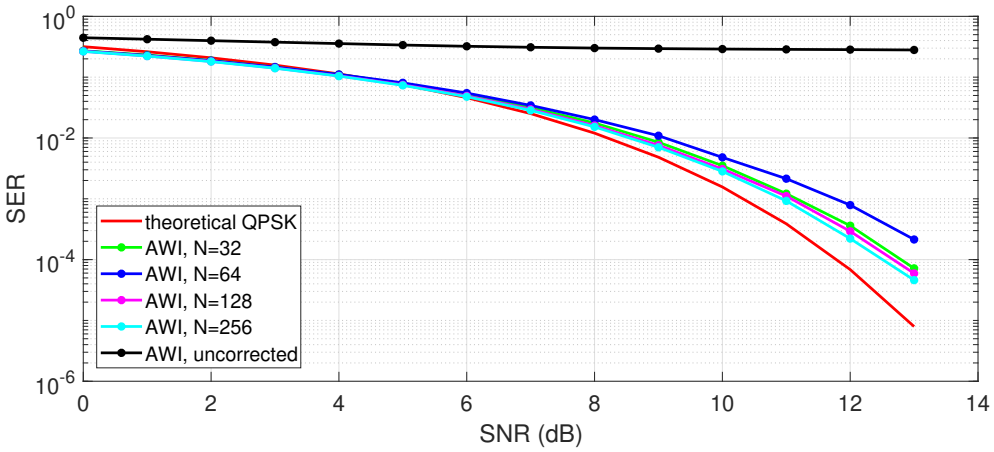

(a) RCR = 20 dB

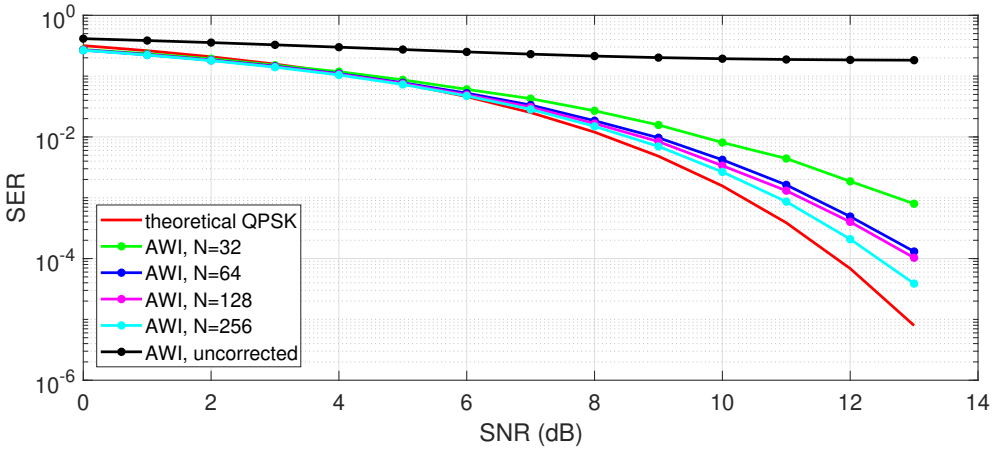

(b) RCR = 10 dB

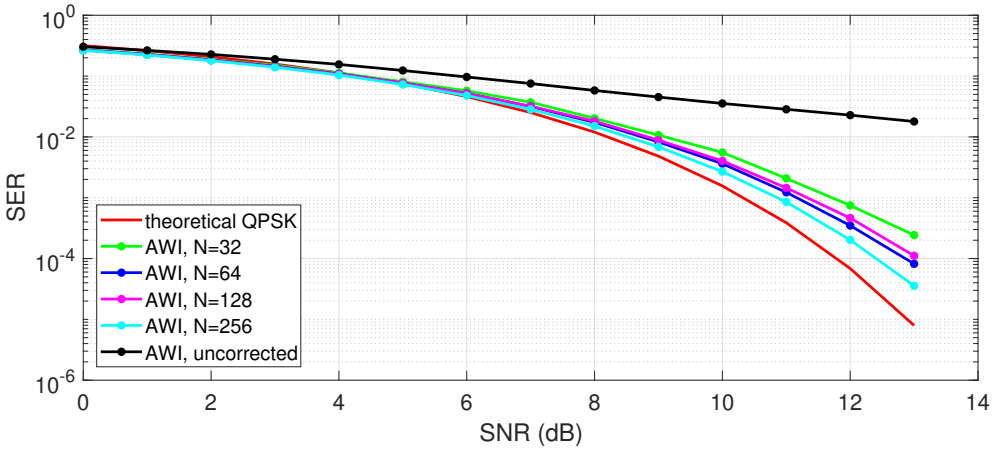

(c) RCR = 5 dB

Figure 4.2. SER vs. SNR (E_s/N_o) for AWI technique for various RCR values.

4.1.2 Using Practical Radar PSD

Again, we examine SERs after interference estimation and corrections for the waterfilling, AWI, and UED communications spectral techniques when using a practical COMNAV radar PSD.

4.1.2.1 Using Waterfilling with Correction

We apply the waterfilling method when the radar utilizes the practical COMNAV radar PSD. As with the Hamming-based radar, the waterfilling method adjusts the number of assigned subcarriers based on the RCR and communications energy constraint. As seen in Table 4.3, the waterfilling method starts with 14 subcarriers for RCR = 0 dB through RCR = 5 dB, decreases to 13 subcarriers for RCR = 10 dB and to 12 subcarriers for RCR = 20 dB. Without estimation and correction, the SER corresponding to RCR = 10 dB has the closest approach to the theoretical QPSK SER. The SERs at RCR = 10 dB and RCR = 20 dB closely approach the theoretical QPSK SER at both low and high values of N by decreasing from 14 subcarriers. SER as a function of SNR is plotted in Figure 4.3 for RCR range of 5, 10, and 20 dB.

Table 4.3. SER performance for waterfilling communications comparing RCR, number of subcarriers, and N symbols collected for correction.

RCR (dB)	Number of Subcarriers	SER at $N = 0$	SER at $N = 32$	SER at $N = 256$
0	14	3.6×10^{-3}	3.8×10^{-4}	2.1×10^{-5}
5	14	3.4×10^{-2}	2.4×10^{-3}	1.6×10^{-4}
10	13	1.7×10^{-3}	2.7×10^{-4}	1.7×10^{-5}
20	12	7.4×10^{-3}	2.8×10^{-4}	1.8×10^{-5}

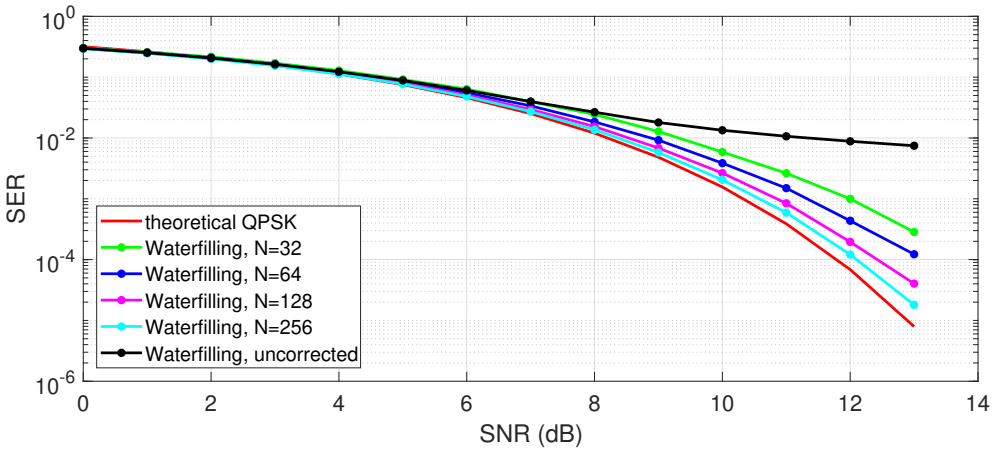

(a) RCR = 20 dB

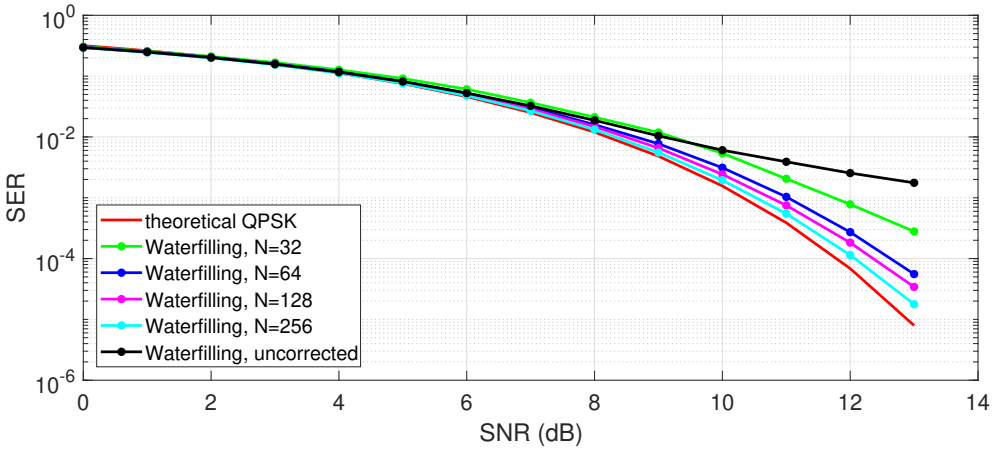

(b) RCR = 10 dB

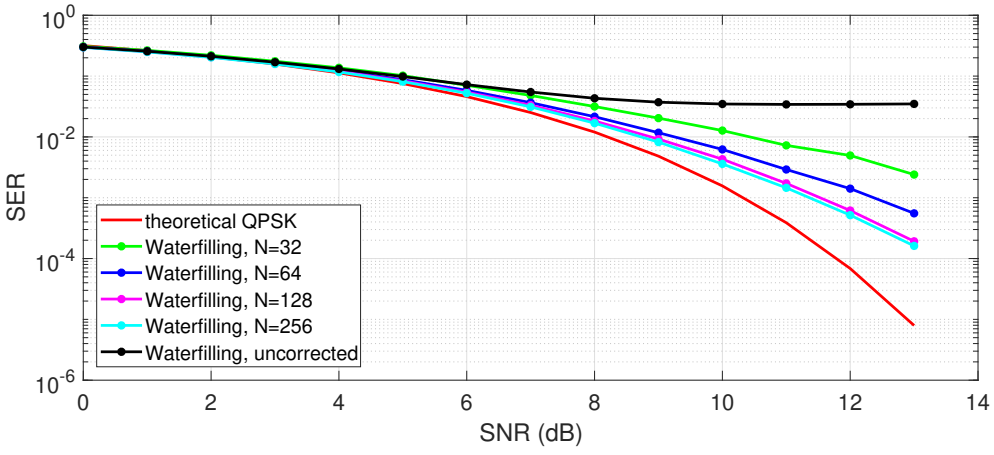

(c) RCR = 5 dB

Figure 4.3. SER vs. SNR (E_s/N_o) for waterfilling technique for various RCR values using practical radar PSD.

4.1.2.2 Using AWI with Correction

We design the AWI method for the practical COMNAV radar PSD to maintain 13 subcarriers, which would provide a throughput increase for RCR = 20 dB over the waterfilling method.

The performance of AWI depends on several factors. The choice of amplitudes for the subcarriers for one is not truly designed to approach the theoretical SER but rather mitigate the symbol errors with spectral shaping where amplitudes are chosen in an adhoc fashion. Indeed, it will be shown that the uncorrected AWI method can actually perform better than with radar interference estimation and subtraction when the RCR is low. In other words, when the radar interference is low enough, correction may not be needed to improve SER with AWI. Indeed, we see in Figure 4.4 (c), for RCR = 5 dB, the AWI SER is the closest to the theoretical SER without the benefit of correction. At $N = 32$, the SER at RCR = 10 dB most closely approaches the theoretical SER as seen in Figure 4.4 (b). Finally at $N = 256$, the SER at RCR = 20 dB outperforms the uncorrected version at $N = 0$ and most closely approaches the theoretical SER for all the values of N as seen in Figure 4.4 (a). This is because the radar interference is so large that estimation and subtraction improve SER significantly. A list involving RCR, number of subcarriers, and SER corresponding to N symbols collected for correction is given in is given in Table 4.4.

Table 4.4. SER performance for AWI communications comparing RCR, number of subcarriers, and N symbols collected for correction.

RCR (dB)	Number of Subcarriers	SER at $N = 0$	SER at $N = 32$	SER at $N = 256$
0	13	1.3×10^{-4}	3.8×10^{-3}	2.8×10^{-4}
5	13	1.1×10^{-4}	2.0×10^{-3}	2.3×10^{-4}
10	13	1.9×10^{-4}	1.5×10^{-3}	2.0×10^{-4}
20	13	1.0×10^{-2}	2.8×10^{-3}	1.8×10^{-4}

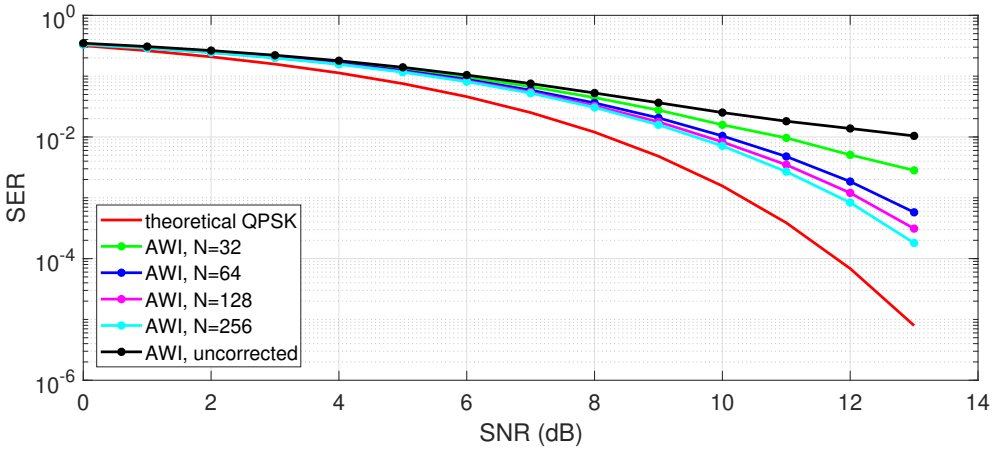

(a) RCR = 20 dB

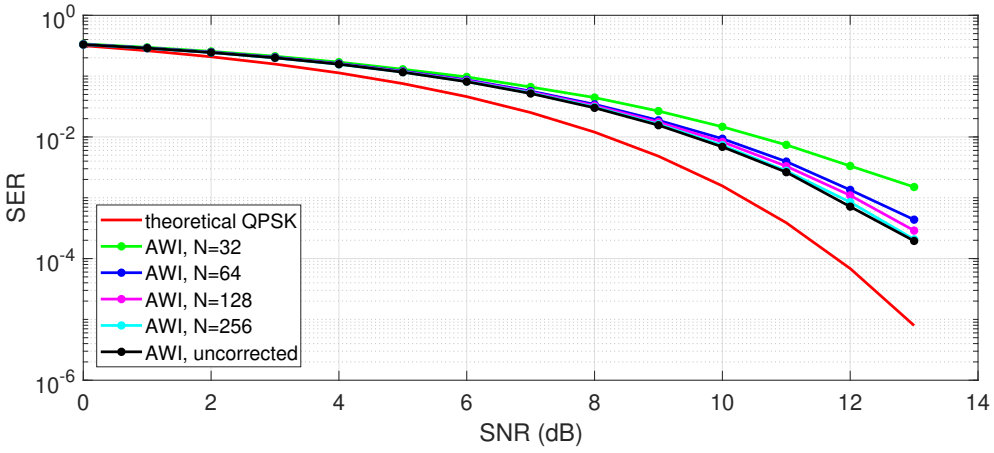

(b) RCR = 10 dB

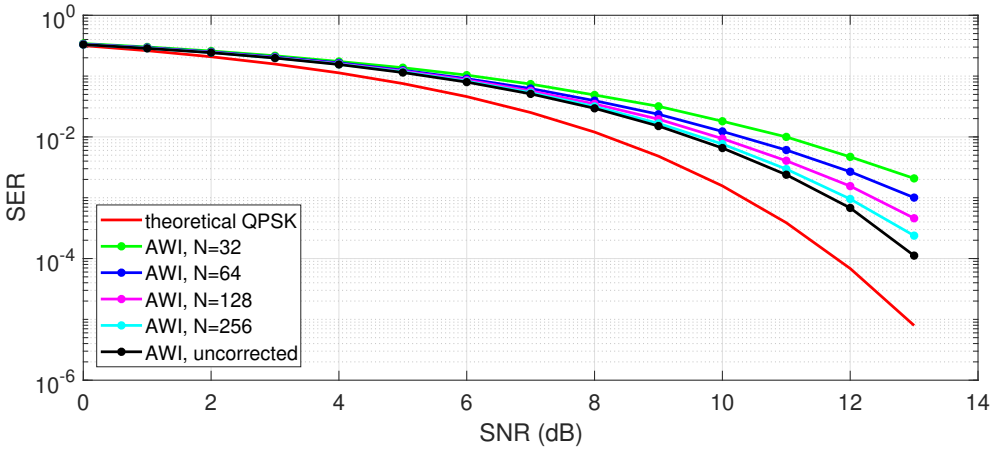

(c) RCR = 5 dB

Figure 4.4. SER vs. SNR (E_s/N_o) for AWI technique for various RCR values using practical radar PSD.

4.1.2.3 Using UED Method

Without regard to the effects on radar performance, we examine the SER when using the entire bandwidth including the radar mainlobe. We assign uniform energy distribution across all 16 subcarriers, dramatically increasing throughput. We see in Figure 4.5 (a) - (c) unimpressive SER performance at all RCRs for uncorrected radar interference at $N = 0$. SERs corresponding to RCR = 0 dB and RCR = 10 dB perform the best at $N = 256$ with similar performance at RCR = 5 dB. SERs corresponding to RCR = 20 dB at $N = 256$ are an order of magnitude lower for the lower RCRs, and despite the increase in radar power, those SERs still outperform SERs with $N = 0$ (no correction) and $N = 32$ at RCR range of $0, 5$, and 10 dB. A list involving RCR, number of subcarriers, and SER corresponding to N symbols collected for correction is given in is given in Table 4.5.

Table 4.5. SER performance for UED communications comparing RCR, number of subcarriers, and N symbols collected for correction.

RCR (dB)	Number of Subcarriers	SER at $N = 0$	SER at $N = 32$	SER at $N = 256$
0	16	6.3×10^{-2}	2.4×10^{-4}	1.4×10^{-5}
5	16	9.4×10^{-2}	2.9×10^{-4}	3.4×10^{-5}
10	16	9.4×10^{-2}	5.0×10^{-4}	1.4×10^{-5}
20	16	1.0×10^{-2}	2.8×10^{-3}	1.8×10^{-4}

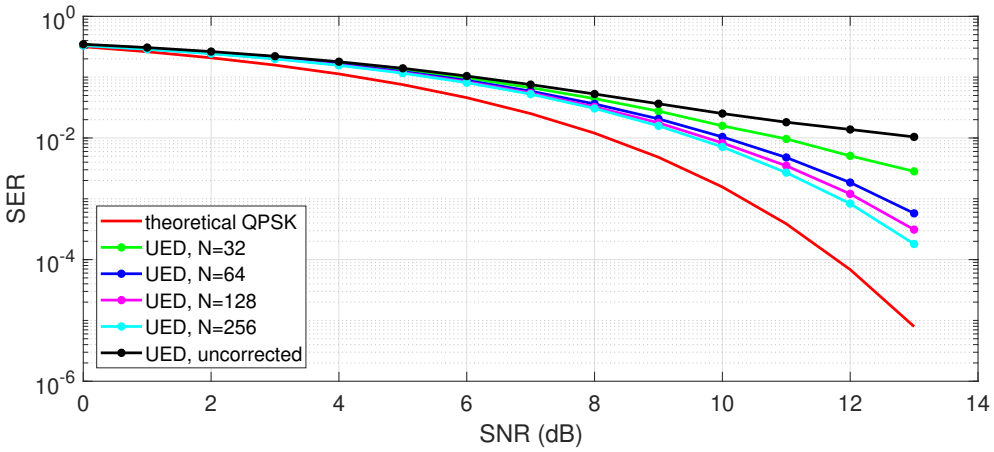

(a) RCR = 20 dB

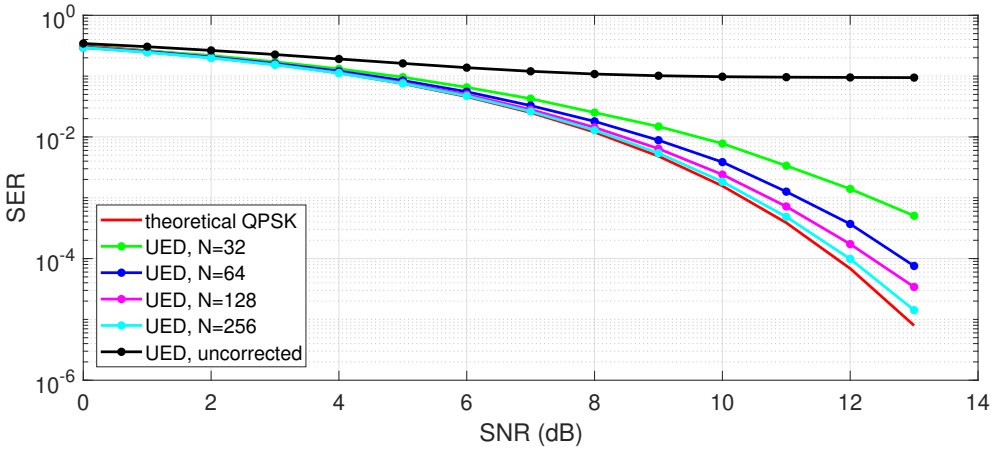

(b) RCR = 10 dB

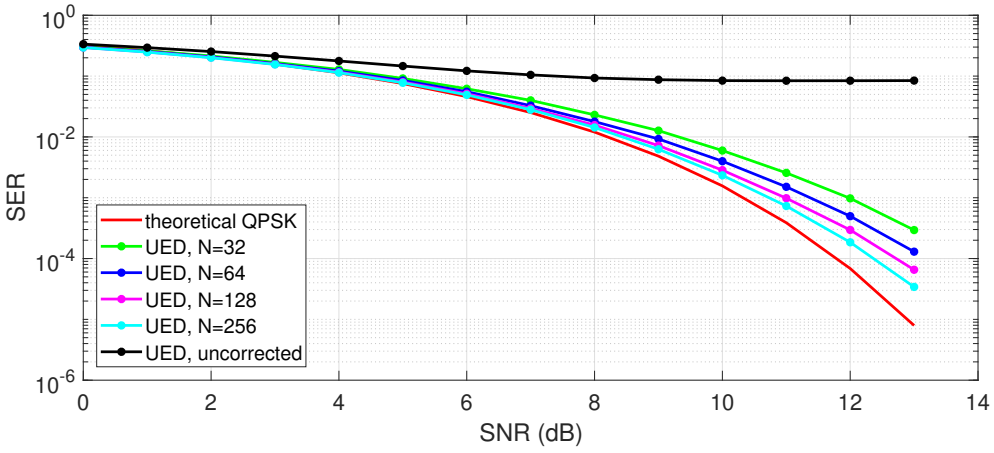

(c) RCR = 5 dB

Figure 4.5. SER vs. SNR (E_s/N_o) for UED technique for various RCR values using practical radar PSD.

4.1.2.4 Analysis of Waterfilling Method against AWI

We compare the SER performance of the waterfilling against the AWI method without regard to throughput in this section.

Comparing the waterfilling method against the AWI method at RCR = 20 dB, we see that the waterfilling method has better performance at $N = 32$ and $N = 256$; however, it has less throughput by assigning 12 subcarriers. The AWI method at $N = 256$ has similar SER performance as the waterfilling method at $N = 32$ with the added benefit of the extra subcarrier. At RCR = 10 dB, both methods maintain 13 subcarriers. The AWI technique, unsurprisingly, has superior performance compared to the waterfilling technique at RCR = 10 dB for $N = 0$. This is due to the fact that the AWI method has less radar interference at subcarrier 5, while the waterfilling technique evenly distributes the signal energy among all the subcarriers, as seen in Figure 4.6 (a). For $N = 256$, the waterfilling method outperforms the AWI method. At RCR = 5 dB, the waterfilling method assigns 14 subcarriers, while the AWI method assigns 13 subcarriers. Similar to RCR = 10 dB, the uncorrected AWI method with RCR = 5 dB ($N = 0$) outperforms the waterfilling method for all values of N. The superior performance with $N = 0$ has the drawback of decreased throughput since the AWI method assigns 13 subcarriers, whereas the waterfilling method (with inferior SER) assigns 14 subcarriers, as seen in Figure 4.6 (b). This indicates that the AWI method achieves superior SER compared to the waterfilling method without the time lag associated with collecting symbols for estimation and subtraction. These results are annotated in Table 4.6.

In Table 4.7 we prioritize throughput, i.e., we want the most throughput with the most desirable SER. At RCR = $0,5$ dB, the waterfilling method assigns 14 subcarriers, yielding the most throughput. By choosing the waterfilling method at RCR = 5 dB with 14 subcarriers instead of the AWI method with 13 subcarriers, as in Table 4.6, we increase the number of symbols collected because the AWI does not require correction at approximately the same SER. At RCR = 10 dB, the waterfilling method assigns 13 subcarriers and provides superior SER over the AWI method, which is consistent with Table 4.6. Finally, at RCR = 20 dB, we choose throughput over SER again. The AWI method provides 13 subcarriers, compared to the waterfilling method with 12 subcarriers. The trade off is a lower SER with the AWI method.

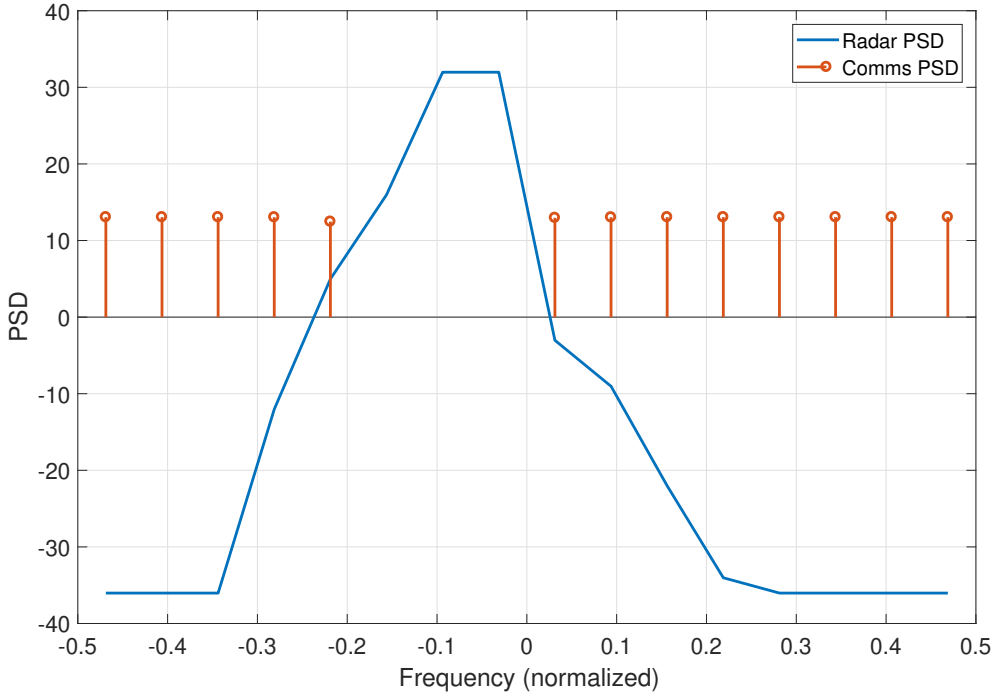

(a) Waterfilling method with 13 OFDM QPSK modulated subcarriers.

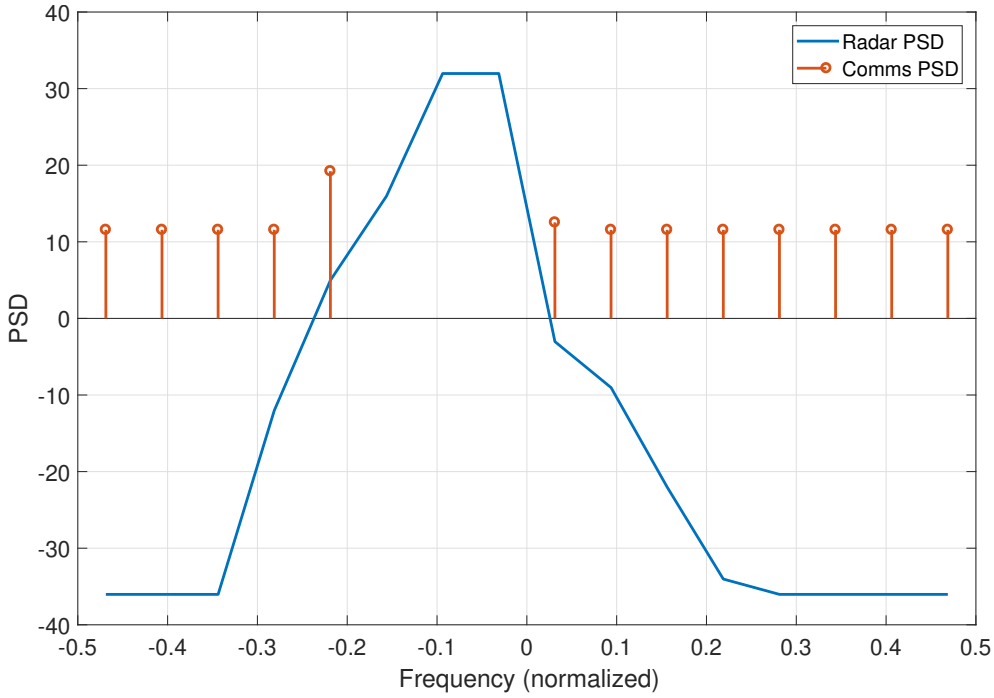

(b) AWI method with 13 OFDM QPSK modulated subcarriers.

Figure 4.6. Downsampled practical radar spectrum with various spectral shaping techniques at RCR = 10 dB and SNR = 13 dB.

Table 4.6. SER performance comparison for waterfilling and AWI communications based on RCR and throughput.

RCR	Spectral Technique	Number of Subcarriers	SER	N
0	Waterfilling	14	2.1×10^{-5}	256
5	AWI	13	1.1×10^{-4}	0
10	Waterfilling	13	1.7×10^{-5}	256
20	Waterfilling	12	1.8×10^{-5}	256

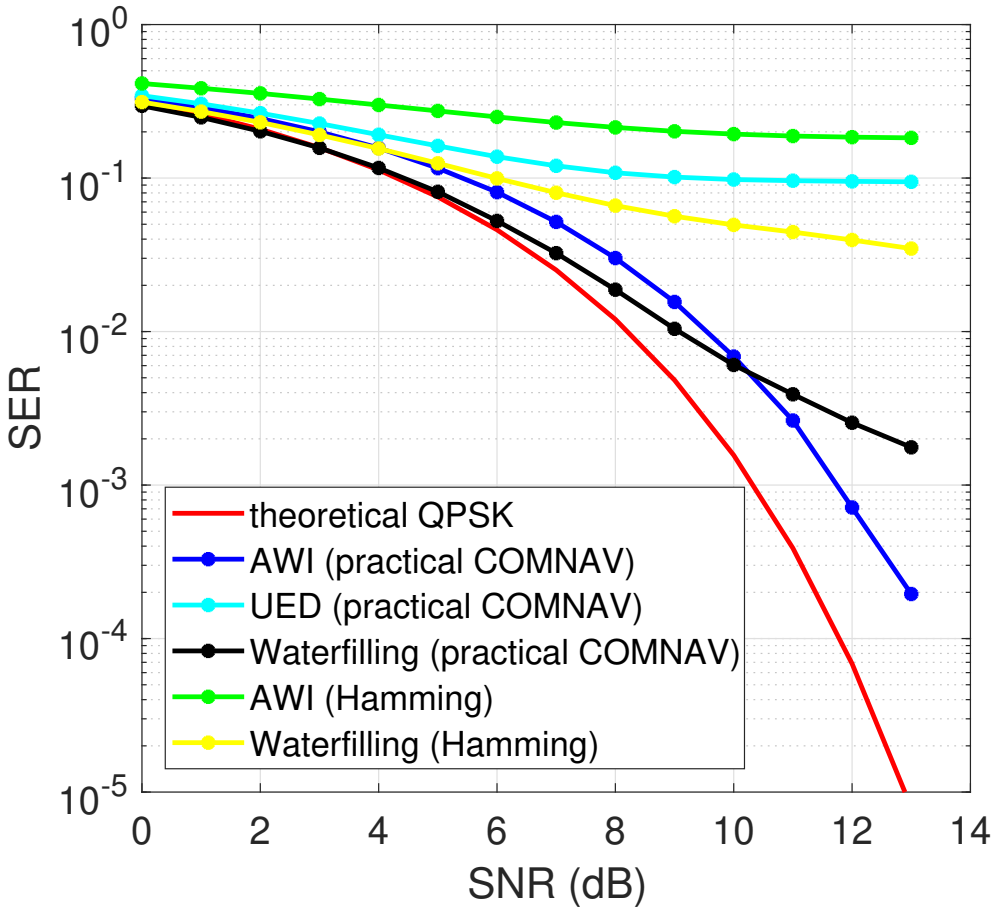

Figure 4.7. SER vs. SNR (E_s/N_o) for $N = 0$ with waterfilling, AWI and UED spectral techniques for practical COMNAV radar PSD and waterfilling and AWI spectral techniques for Hamming-based radar PSD for RCR = 10 dB.

Table 4.7. SER performance comparison for waterfilling and AWI communications based on RCR and throughput.

RCR	Spectral Technique	Number of Subcarriers	SER	N
0	Waterfilling	14	2.1×10^{-5}	256
5	Waterfilling	14	1.6×10^{-4}	256
10	Waterfilling	13	1.7×10^{-5}	256
20	AWI	13	1.8×10^{-4}	256

4.1.2.5 Analysis for All Spectral Shaping Methods Utilizing the Practical Radar PSD

Now we compare the SERs for all three spectral techniques when the radar utilizes the practical COMNAV PSD while considering time latency without regard to throughput. As designed, the UED method uses the entire bandwidth (maximum throughput), so instead we analyze which frequency shaping technique yields the best SER in Table 4.8 if we consider time latency. At $N = 0$, our top performers are AWI and waterfilling. This remains the same as in previous analysis. At $N = 32$, the UED method yields superior SERs at RCR = 0 dB and RCR = 5 dB, whereas waterfilling performs better at RCR = 10 dB and RCR = 20 dB. At $N = 256$, the UED method has the best performance for RCR range of $0, 5$, and 10 dB, and the waterfilling method most closely approaches the theoretical SER at RCR = 20 dB. From Table 4.8 we see that if time latency is not a priority, i.e., we allow for larger number of symbols for estimation and correction, then we can increase throughput at the lower RCRs.

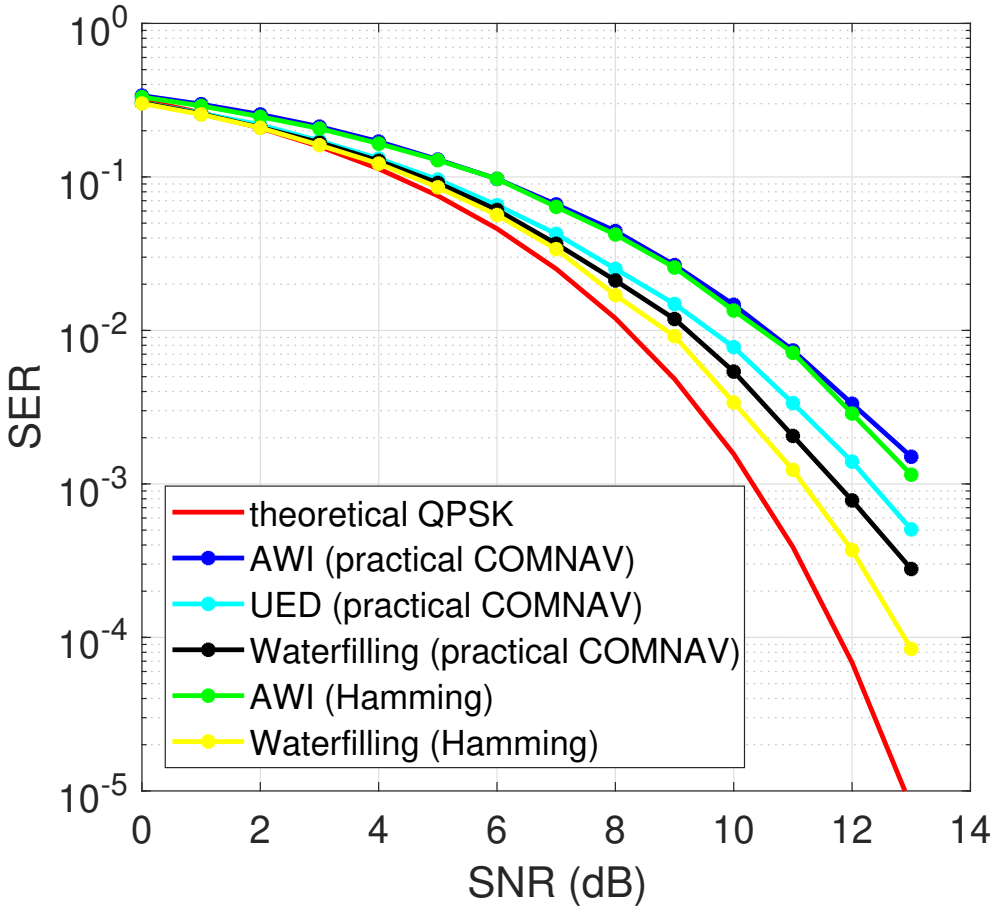

Figure 4.8. SER for $N = 32$ with waterfilling, AWI and UED spectral techniques for practical COMNAV radar PSD and waterfilling and AWI spectral techniques for Hamming-based radar PSD for RCR = 10 dB and SNR = 10 dB.

Table 4.8. Best SER performance among waterfilling, AWI, and UED techniques based on RCR and time latency.

RCR	Spectral Technique, $N = 0$	Spectral Technique, $N = 32$	Spectral Technique, $N = 256$
0	AWI	UED	UED
5	AWI	UED	UED
10	AWI	Waterfilling	UED
20	Waterfilling	Waterfilling	Waterfilling

4.1.3 Analysis for All Spectral Shaping Methods

We compare the spectral shaping techniques using the Hamming-based radar PSD (i.e., waterfilling and AWI) against the spectral techniques using the practical COMNAV radar PSD (i.e., waterfilling, AWI, and UED) to identify the best SER. We fix the required number of received subcarrier symbols and compare SERs. Throughput is not a consideration since the UED method maximizes the subcarrier injections across the radar mainlobe.

4.1.3.1 SER for All Spectral Shaping Methods with $N = 0$

We first consider the uncorrected case, where $N = 0$. The AWI and waterfilling techniques using the practical radar PSD perform the best, followed by the waterfilling technique for the Hamming-based radar PSD, UED for the practical radar PSD, and finally the AWI technique for the Hamming-based radar PSD as annotated in Table 4.9. The uncorrected SERs vs. SNR for all five spectral shaping techniques are depicted in Figure 4.7 at RCR = 10 dB.

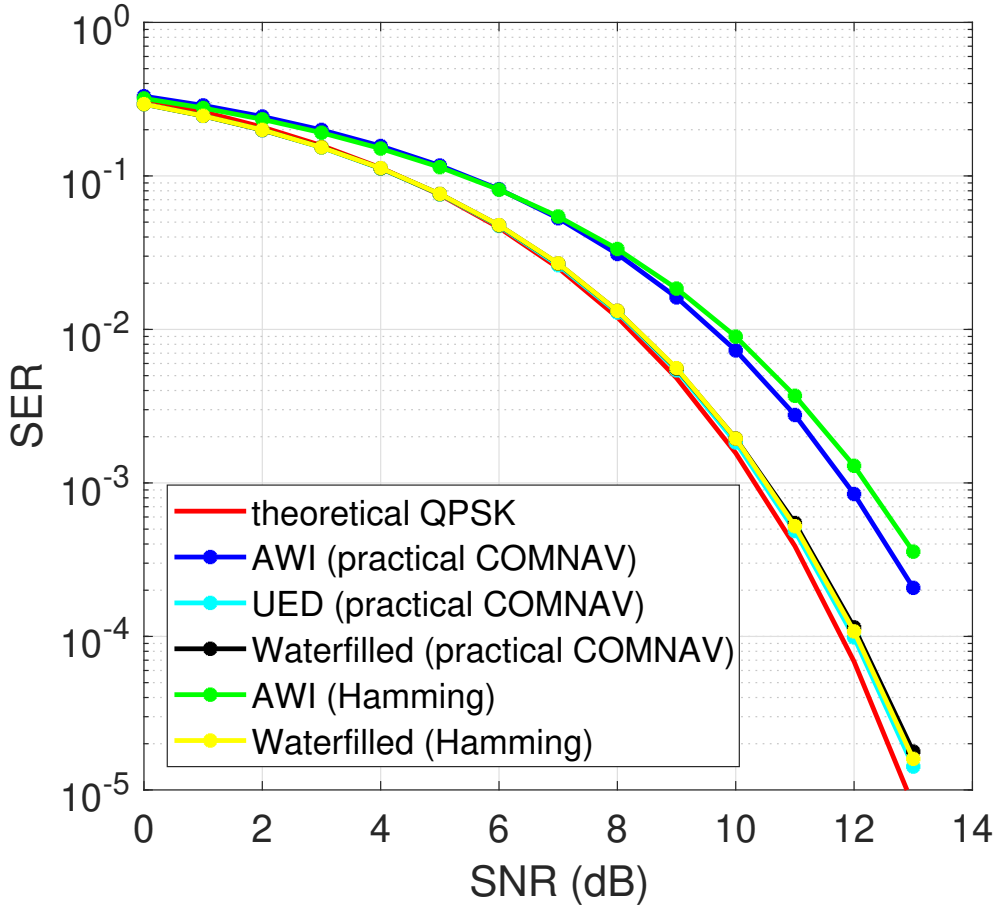

Figure 4.9. SER for $N = 256$ with waterfilling, AWI and UED spectral techniques for practical COMNAV radar PSD and waterfilling and AWI spectral techniques for Hamming-based radar PSD for RCR = 10 dB.

4.1.3.2 SER for All Spectral Shaping Methods with $N = 32$

Next, we examine the case using $N = 32$ received symbols per interfered subcarrier for estimation and subtraction. The waterfilling techniques for Hamming-based and practical radar PSDs perform the best, respectively, in terms of SER, followed by UED for the practical radar, AWI for the Hamming-based radar PSD, and AWI for the practical radar PSD as seen in Figure 4.8. Notably, the AWI for the practical radar PSD, which has the best SER at $N = 0$, now has the worst SER performance with $N = 32$. From Table 4.4, we see that the AWI method at RCR = 10 dB performs better at $N = 0$ than it does at $N = 32$, (i.e., corrections do not improve the SER for this particular case). The other spectral shaping

techniques have successful corrections and explains the AWI technique's inferior SER to the other spectral shaping methods at $N = 32$.

4.1.3.3 SER for All Spectral Shaping Methods at $N = 256$

Finally, using $N = 256$ received symbols per interfered subcarrier for estimation and subtraction, the UED technique for the practical radar PSD performs the best. The top performers at $N = 256$ include UED for the practical radar and the waterfilling methods for both radar PSDs. These very closely approximate the theoretical SER for QPSK as seen in Figure 4.9. The AWI method for the practical radar and the AWI method for the Hamming-based radar follow.

At $N = 0$, the AWI method using the practical radar PSD has a similar performance as waterfilling method at $N = 32$, implying that time or latency issues can be overcome by sacrificing some errors. At $N = 32$ and $N = 256$, the waterfilling methods consistently outperform the AWI methods using estimation and subtraction. As the collected received symbols increase, the estimation and correction for UED substantially improve the SER as evidenced by the order of magnitude improvement from $N = 32$.

Table 4.9. Best SER performance for all spectral shaping techniques based on RCR = 10 dB, SNR = 10 dB, and symbol latency N.

Spectral Technique, $N = 0$	Spectral Technique, $N = 32$	Spectral Technique, $N = 256$
AWI (COMNAV)	Waterfilling (Hamming)	UED (COMNAV)
Waterfilling (COMNAV)	Waterfilling (COMNAV)	Waterfilling (Hamming)
Waterfilling (Hamming)	UED (COMNAV)	Waterfilling (COMNAV)
UED (COMNAV)	AWI (Hamming)	AWI (COMNAV)
AWI (Hamming)	AWI (COMNAV)	AWI (Hamming)

4.2 Probability of Detection and MDR

Next, we investigate the communications waveform effect of injecting subcarriers on the radar's percentage or probability of detection P_D. The theoretical P_D [12] is given by

$$P_D = Q\left(Q^{-1}\left(P_{FA}\right) - \sqrt{\frac{2E_r}{\sigma^2}}\right) \tag{4.1}$$

where $Q(\bullet)$ denotes the Q-function, $Q^{-1}(\bullet)$ denotes the inverse Q-function, P_{FA} is probability of false alarm, and E_r is the received radar energy. In order to visually see the slight differences in P_D, we define the MDR to be $1 - P_D$ and use it as a metric of performance to compare the effects of the spectral shaping techniques on the radar PSDs.

4.2.1 MDR for the Hamming-Based Radar

We examine the encroaching OFDM subcarriers' effects on a Hamming-based radar at RCR = 0, 10 dB and expect very little deviation from the theoretical P_D by examining the MDR. We show that due to the minimal communications interference on the radar both spectral shaping techniques minimally affect the radar's MDR. We see in both panels of Figure 4.10 that both the MDRs for waterfilling and AWI methods follow the theoretical MDR closely at RCR = 10 dB. At RCR = 0 dB the radar performance slightly degrades at higher radar SNR (E_r/σ^2). In Figure 4.10 (b), it is easy to distinguish that the waterfilling method affects the MDR slightly worse than the AWI method.

4.2.2 MDRs for the Practical Radar PSD

Again, we examine the encroaching OFDM subcarriers' effects on the practical COMNAV radar PSD.

4.2.2.1 WF vs. AWI vs. UED

Similarly, the waterfilling and AWI communications techniques minimally interfere with the practical radar PSD as shown in Figure 4.11 (a) and (b). As expected, the UED method injects substantial communications interference on the radar at RCR = 0 dB at both $P_{FA} = 10^{-1}$ and $P_{FA} = 10^{-3}$. In Figure 4.11, we see a similar MDR degradation from the UED method compared to the AWI and waterfilling at RCR = 10 dB.

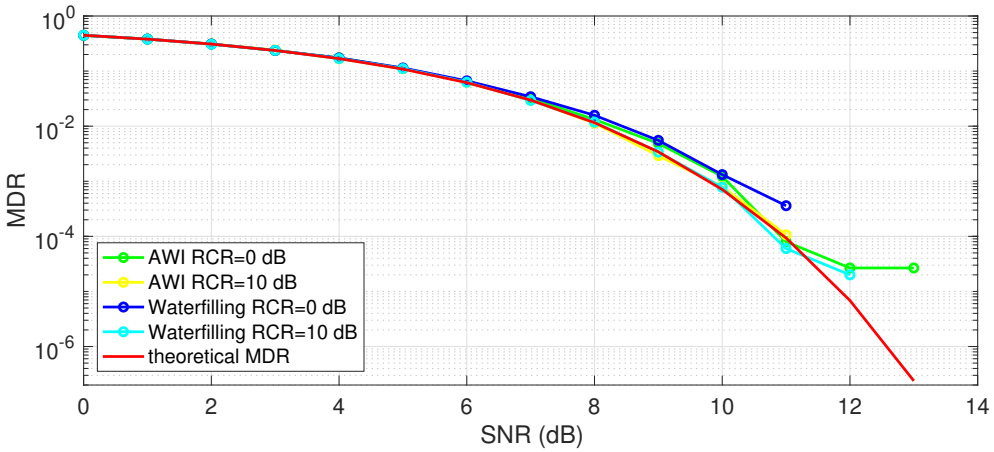

(a) $P_{FA} = 10^{-1}$

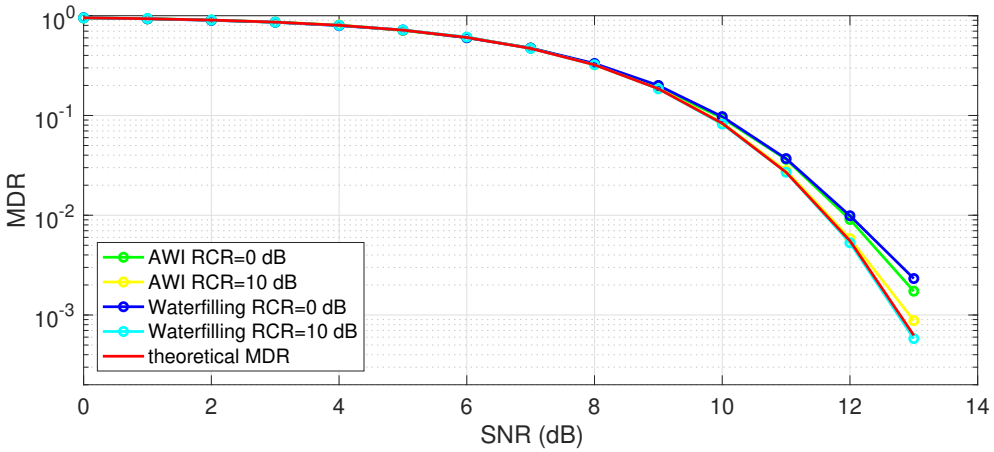

(b) $P_{FA} = 10^{-3}$

Figure 4.10. MDR vs. radar SNR (E_r/σ^2) for waterfilling and AWI communications waveforms at RCR = 0 dB and RCR = 10 dB at $P_{FA} = 10^{-1}$ and $P_{FA} = 10^{-3}$.

4.2.2.2 UED with Increasing Subcarrier-Radar Mainlobe Overlap

Next, we investigate the effects of increasing communications interference on the radar performance by systematically adding subcarriers one at a time. We start with 12 subcarriers, which has minimal interference on the radar PSD. We see in Figure 4.12 (a) and (b) and in Figure 4.13 (a) and (b) that the MDR in the trivial case follows the theoretical the MDR very closely. As we increase the number of subcarriers injected into the radar mainlobe, radar performance degrades. This is evident in the case of RCR = 0 dB using subcarriers with equal magnitude.

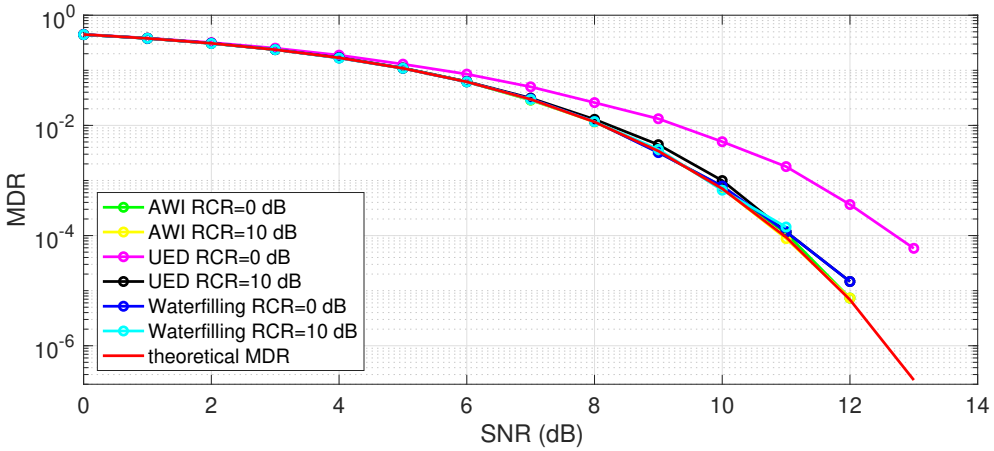

(a) $P_{FA} = 10^{-1}$

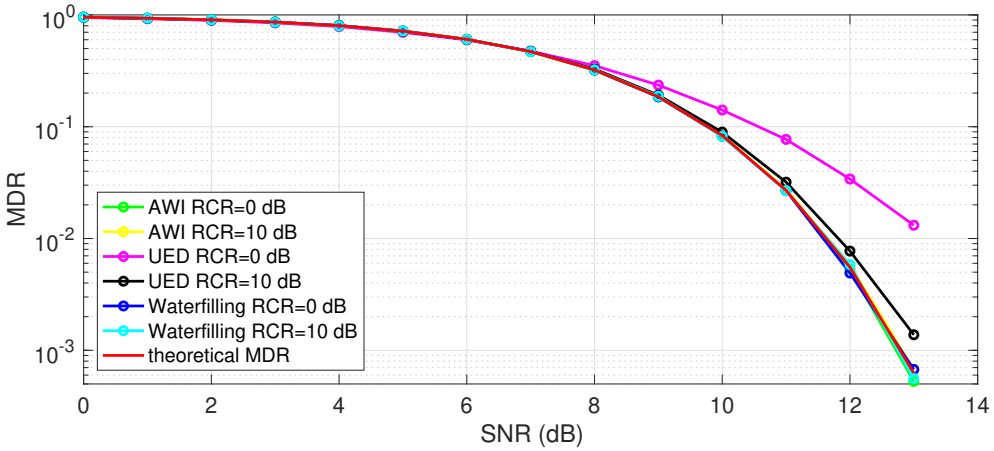

(b) $P_{FA} = 10^{-3}$

Figure 4.11. MDR vs. radar SNR (E_r/σ^2) for waterfilling, AWI, and UED communications waveforms at RCR = 0 dB and RCR = 10 dB calculated at $P_{FA} = 10^{-1}$ and $P_{FA} = 10^{-3}$.

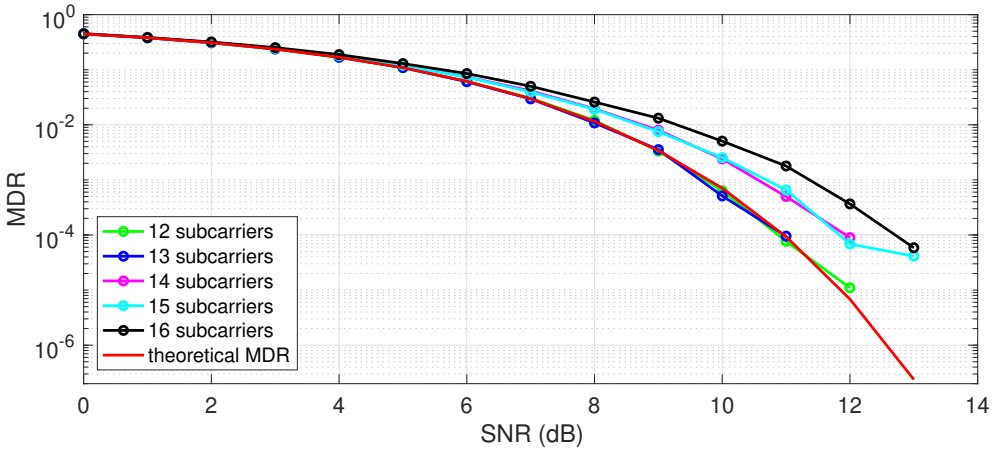

(a) RCR = 0 dB

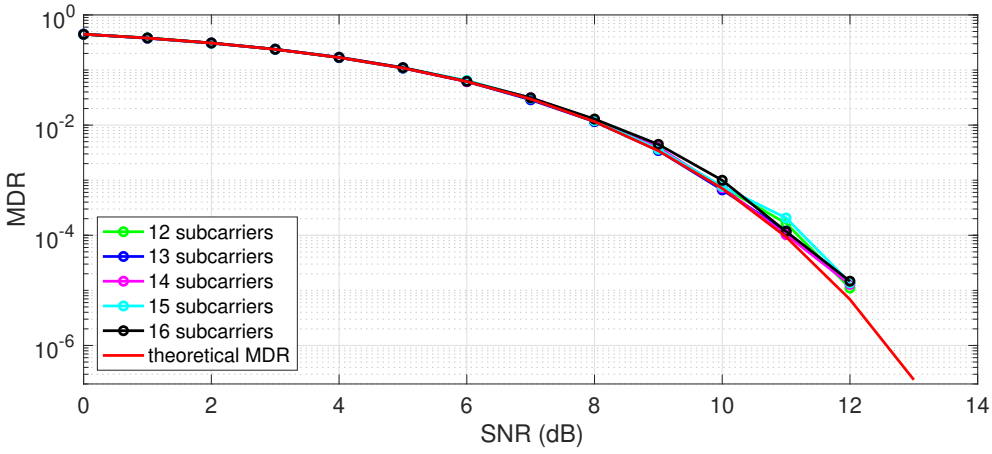

(b) RCR = 10 dB

Figure 4.12. MDR vs. radar SNR (E_r/σ^2) for UED communications waveform calculated at $P_{FA} = 10^{-1}$ at RCR = 0 dB and RCR = 10 dB as a function of increasing subcarriers inside the radar mainlobe.

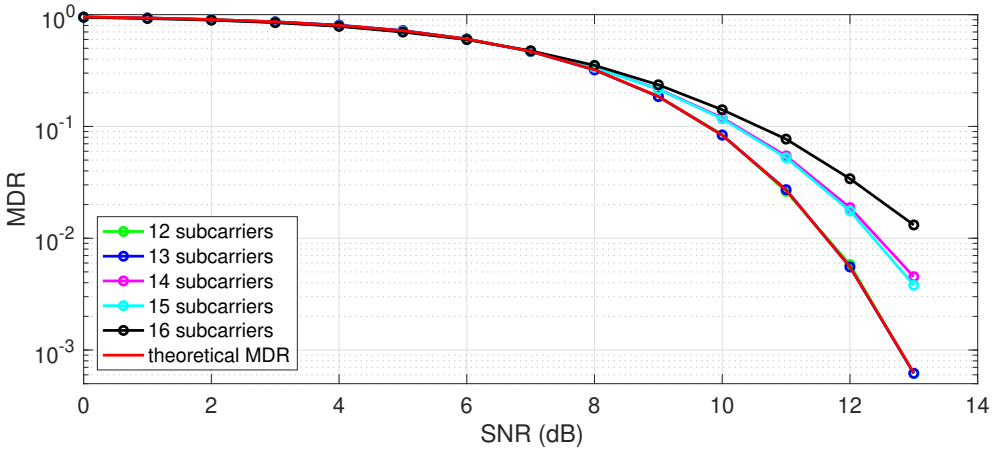

(a) RCR = 0 dB

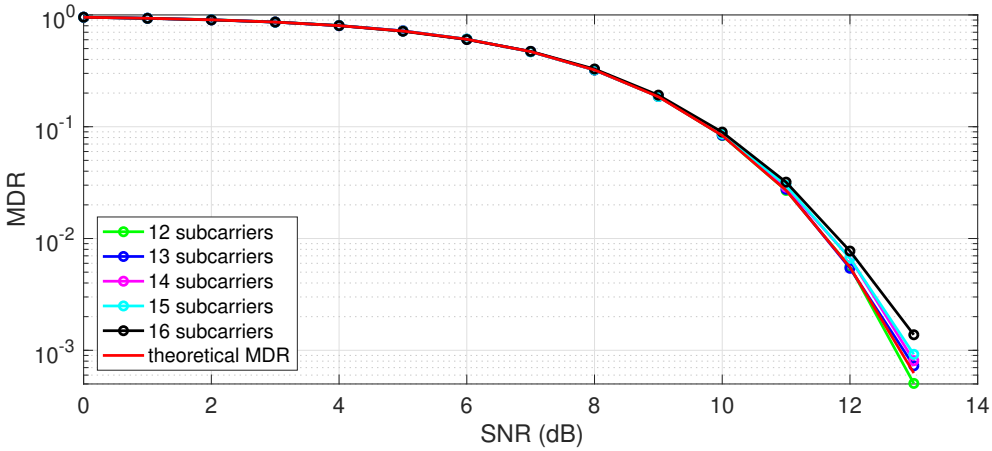

(b) RCR = 10 dB

Figure 4.13. MDR vs. radar SNR (E_r/σ^2) for UED communications waveform calculated at $P_{FA} = 10^{-3}$ at RCR = 0 dB and RCR = 10 dB as a function of increasing subcarriers inside the radar mainlobe.

CHAPTER 5:
Conclusions

We summarize our work and propose future research ideas in the field of spectrum sharing for radar-communications systems.

5.1 Summary

In this work, we investigated exploiting radar guard bands for communications with the extra motivation to increase throughput. We utilized waterfilling and AWI techniques to design an OFDM spectral shape to increase throughput with the use of radar's guard bands and injecting a few subcarriers into its mainlobe. Unfortunately, in several cases, the radar's large power interferes with the injected subcarriers such that the SERs are highly degraded. By using estimation in the receiver, we corrected the interference prior to demodulating the communications waveform. By changing the SNR, RCR, and number of symbols N collected for correction, different spectral shaping techniques provided the most desirable SER. We found at RCR = 10 dB and SNR = 13 dB that the AWI for the practical COMNAV radar PSD achieved the best SER for $N = 0$ (i.e., the uncorrected case). At the same RCR and SNR for $N = 32$, the waterfilling method for both radar PSDs achieved the best SER. Finally, for $N = 256$, the UED method for the practical COMNAV radar PSD achieved the best SER. By using more symbols for estimation of the radar signal in the injected subcarriers, we improved SER performance for waterfilling and UED considerably. The AWI method reached a point where it could no longer correct radar interference regardless of higher values of N. In conclusion, we showed the possibility of injecting OFDM communications inside the guard bands and mainlobe of a radar PSD and, by doing so, increasing the communications throughput with minimal and/or acceptable effect on radar MDR.

5.2 Future Work

There are three opportunities for research not addressed in this work. First, hardware co-simulation in a field programmable gate array (FPGA) of communications modulation and demodulation in the presence of practical COMNAV radar interference. Second, examining

the effects of interference to include inter-symbol interference (ISI) and incorporating cyclic prefixes for the OFDM signal. Finally, examining the effect of radar rotation and antenna gain as seen by the communications device with the potential to increase throughput.

List of References

[1] A. R. Chiriyath, B. Paul and D. W. Bliss, "Radar-communications convergence: Coexistence, cooperation, and co-design," *IEEE Transactions on Cognitive Communications and Networking*, vol. 3, no. 1, pp. 1-12, March 2017. doi: 10.1109/TCCN.2017.2666266

[2] C. Sturm and W. Wiesbeck, "Waveform design and signal processing aspects for fusion of wireless communications and radar sensing," *Proceedings of the IEEE*, vol. 99, no. 7, pp. 1236-1259, July 2011. doi: 10.1109/JPROC.2011.2131110

[3] A. Khawar, A. Abdel-Hadi and T. C. Clancy, "MIMO radar waveform design for coexistence with cellular systems," *IEEE International Symposium on Dynamic Spectrum Access Networks*, McLean, VA, 2014, pp. 20-26. doi: 10.1109/DySPAN.2014.6817775

[4] R. Saruthirathanaworakun, J. M. Peha and L. M. Correia, "Opportunistic sharing between rotating radar and cellular," *IEEE Journal on Selected Areas in Communications*, vol. 30, no. 10, pp. 1900-1910, November 2012. doi: 10.1109/JSAC.2012.121106

[5] S. D. Blunt, P. Yantham, "Waveform design for radar-embedded communications," *2007 International Waveform Diversity and Design Conference*, Pisa, 2007, pp. 214-218. doi: 10.1109/WDDC.2007.4339413

[6] G. Meager, R. A. Romero, Z. Staples, "Estimation and cancellation of high powered radar interference for communication signal collection," *IEEE Radar Conference*, Philadelphia, PA, 2016, pp. 1-4. doi: 10.1109/RADAR.2016.7485263

[7] A. Hunt, R. A. Romero, Z. Staples, "The effect of embedded intrapulse communications on pulsed radar probability of detection," *IEEE Global Conference on Signal and Information Processing*, Montreal, QC, 2017, pp. 348-352. doi: 10.1109/GlobalSIP.2017.8308662

[8] E. J. Bittner, "Covert half duplex data link using radar-embedded communications with various modulation schemes," M.S. thesis, Dept. of Elec. and Comp. Eng., Naval Postgraduate School, Monterey, CA, USA, 2017.

[9] J. D. Hooper, "Practical maritime waveform considerations to operationalize radar embedded communications," M.S. thesis, Dept. of Elec. and Comp. Eng., Naval Postgraduate School, Monterey, CA, USA, 2018.

[10] K. D. Shepherd, R. A. Romero, "Radar waveform design in active communications channel," *Asilomar Conference on Signals, Systems and Computers*, Pacific Grove, CA, 2013, pp. 1515-1519. doi: 10.1109/ACSSC.2013.6810549

[11] M. R. Bell, "Information theory and radar waveform design," *IEEE Transactions on Information Theory*, vol. 39, no. 5, pp. 1578-1597, 1993. doi: 10.1109/18.259642

[12] S. M. Kay, *Fundamental of Statistical Signal Processing, Vol. II, Detection Theory*, Upper Saddle River, NJ, USA: Prentice-Hall PTR, 1998.

[13] B. Sklar, *Digital Communications Fundamentals and Applications*, Upper Saddle River, NJ, USA: Prentice-Hall PTR, 2001.

Initial Distribution List

1. Defense Technical Information Center
   Ft. Belvoir, Virginia

2. Dudley Knox Library
   Naval Postgraduate School
   Monterey, California